energies

MDPI

*Article*

# Novel Planning Methodology for Spatially Optimized RES Development Which Minimizes Flexibility Requirements for Their Integration into the Power System

**Bojana Škrbić * and Željko Đurišić**

School of Electrical Engineering, University of Belgrade, 11000 Belgrade, Serbia
* Correspondence: bskrbic@etf.bg.ac.rs

**Abstract:** An optimization model which determines optimal spatial allocation of wind (WPPs) and PV power plants (PVPPs) for an energy independent power system is developed in this paper. Complementarity of the natural generation profiles of WPPs and PVPPs, as well as differences between generation profiles of WPPs and PVPPs located in different regions, gives us opportunity to optimize the generation capacity structure and spatial allocation of renewable energy sources (RES) in order to satisfy the energy needs while alleviating the total flexibility requirements in the power system. The optimization model is based on least squared error minimization under constraints where the error represents the difference between total wind and solar generation and the referent consumption profile. This model leverages between total energy and total power requirements that flexibility resources in the considered power system need to provide in the sense that the total balancing energy minimization implicitly bounds the power imbalances over the considered time period. Bounding the power imbalances is important for minimizing investment costs for additional flexibility resources. The optimization constraints bound the installed power plant capacity in each region according to the estimated technically available area and force the total energy production to equal the targeted energy needs. The proposed methodology is demonstrated through the example of long-term RES planning development for complete decarbonization of electric energy generation in Serbia. These results could be used as a foundation for the development of the national energy strategy by serving as a guidance for defining capacity targets for regional capacity auctions in order to direct the investments in wind and solar power plants and achieve transition to dominantly renewable electricity production.

**Keywords:** decarbonization; RES capacity expansion planning; flexibility; optimization; constrained least squares



**Citation:** Škrbić, B.; Đurišić, Ž. Novel Planning Methodology for Spatially Optimized RES Development Which Minimizes Flexibility Requirements for Their Integration into the Power System. *Energies* **2023**, *16*, 3251. https://doi.org/10.3390/en16073251

Academic Editors: Yuqing Bao, Zhenya Ji and Zhenyu Lv

Received: 9 March 2023
Revised: 27 March 2023
Accepted: 29 March 2023
Published: 5 April 2023



## 1. Introduction

Sustainable development requires an urgent reduction in carbon emissions into the atmosphere on a global level in order to combat global warming [1–3]. The electricity sector is one of the main contributors of carbon emissions due to the significant share of fossil fuel thermal power plants in electricity generation in most power systems. Coal-fired power plants provided 36% of global electricity generation in 2021 [4]. Besides climate change impact, fossil fuel thermal power plants cause local air pollution which raises health concerns and ecosystem hazards. These problems are becoming more pronounced due to the extinction of coal reserves, which brings lower-quality coal into use. The combustion of lower quality coal increases specific carbons emissions of a power plant. By the introduction of carbon trading and green certificate mechanisms the decarbonization process becomes economically motivated also since fossil fuel power plants face additional production costs due to carbon emissions [5]. The phasing out of fossil fuel thermal power plants in the future is inevitable and substitute sustainable energy sources have to be developed [1,4,6,7].

Variable RES such as WPPs and PVPPs, are intensively being developed around the world in order to substitute the conventional thermal power plant (TPP) generation [8,9]. This process needs to take into account technical, ecological, economic and security aspects; therefore, there is a need for suitable national strategies for the development of RES and the accompanying capacities that should provide equilibrium between the generated and the consumed electric energy at all time scales and capacities that should provide the regulation of frequency and scheduled power exchanges. The main challenge is the variability in RES generation. The WPP and PVPP generations are not dispatchable because they depend on the availability of the primary energy resources (wind and irradiation). This brings a number of operational planning issues in power systems with high variable RES penetration levels [10]. However, the complementarity or synergy of the wind and PV energy availability, which exists in almost all regions in the world [11,12], is a favorable feature of these energy sources that should be taken advantage of when planning the optimal structure of generating capacities in national energy systems. The main challenge is to maintain equality between the generated active power and the consumed active power by unit commitment and dispatching of suitable balancing capacities through operational planning for different time scales (yearly, monthly, weekly, daily, and even intra-daily). The construction and operation in reserve of flexible generation and storage capacities needed for balancing the generation and consumption significantly affect the price of electric energy [10,13]. Besides the investment costs for developing balancing capacities and their impact on the environment, the process of energy storage is accompanied by certain energy losses which can significantly affect the efficiency of electric power system. Therefore, it is important to plan the development of RES so that the need for constructing and employing storage capacities would be as small as possible. This means that the assessment of the power system's flexibility requirements is inseparable from the planning of RES development for large penetration level scenarios. On the other hand, the certain RES development scenario requires suitable development of the network infrastructure. Therefore, the required transmission system network development can also affect how RES will be developed.

Optimal generation expansion planning is a very current topic in almost all countries and regions. Many national energy system studies are being conducted in order to find the optimal generation mix under conditions of large RES penetration. Some of them can be found in [14–27]. The most recent research on long-term electricity resource planning models is concerned with including operational aspects (generation constraints regarding ramping, minimum stable output levels, cycling costs, operating reserves) [14,15,28–35], transmission network expansion [14–16,26,36], environmental policy requirements [15,17,24], higher temporal resolution of chronologically ordered generation and consumption data [15,26,34,36,37], and modelling linkages between the electricity and the transportation and heating sectors [17,25,38] with different levels of detail depending on the planning goal and the computational tractability of the problem. These models determine the electricity generation and storage investments and operating decisions to meet forecasted electricity demand reliably over the course of a future time period which minimize the total investment and operation costs while satisfying the imposed operational and environmental constraints. The obtained expansion plans are inevitably dependent on long-term assumptions regarding the future technology and primary fuel costs. These expansion plans result in spatial concentration of WPPs and PVPPs in locations with the best wind and PV energy potential [39–42]. While this is well aligned with investors' interests, it differs from a spatially optimal allocation from society's point of view since RES production also has adverse environmental impacts, such as loss of biodiversity and disturbances to humans [39]. Social welfare (economic efficiency achieved by minimizing the total social cost which comprises the private costs borne by private investors and external cost reflecting the impact of RES on the environment) and equity (even distribution of the burdens of RES generation across all individuals of society) are considered to plan spatially distributed RES in [39]. In paper [43] numerous scenarios are generated by linking two optimization models:

EXPANSE [42] and PyPSA [44], and applying the modeling to generate alternatives (MGA) technique [45] and compared based on the system costs and their spatial distribution. The results show that in between the scenarios which minimize system costs and the scenarios which maximize regional equity, stand the RES development scenarios which maximize RES generation [43]. These scenarios result in higher system costs but contribute to the reduction in inter-regional differences. In the recent literature, different tools, algorithms and optimization techniques are applied for solving the problem of planning the optimal structure of generation capacities in national energy systems [46]. Paper [47] gives a review of planning studies and methodologies used for determination of optimal generation capacity mix in cases of high shares of PV and wind. This review paper shows that very few studies have implemented the assessment of the power system flexibility in their planning model. One of the most used tools to perform energy planning and support energy decision makers is EnergyPLAN [48], which does not model flexibility requirements. Energy models which incorporate modelling of flexibility requirements are the models implemented in commercial software such as TIMES [49], OSeMOSYS [50] and PLEXOS [51]. National-scale energy system optimization models (ESOMs) are usually modeled as single-region systems which use aggregated representation of energy resources, as in [14,16–25,27]. In [14], the generation and transmission expansion planning model, which includes an effective embedded linear relaxation of the unit commitment problem and representative days, is used to find the optimal RE mix which minimizes both investment and operational costs over a planning horizon divided into discrete planning periods. The model is demonstrated for different decarbonization scenarios for the Chilean power system. This model is based on several extensions and modifications of the SWITCH-Model [52] and solved using Gurobi [53]. Gurobi is used for solving energy models formulated as linear optimization problems in [16,17]. In [16], a generation expansion planning model which includes unit commitment and uses clustered representative days is used for investigating optimal decarbonization pathways for the United Kingdom. Decarbonization of the Croatian energy system (power, industry, heat and transportation sectors) is analyzed in [17] using H2RES modelling software [54]. In [18], an optimal energy mix planning model for the Korean power system was calculated using Evolver software [55], which is a robust commercial optimization code based on hybrid scatter–genetic algorithm. In [19], the long-range energy alternatives planning model for investigating optimal power generation structure in South Korea for different energy and climate change policy scenarios is given. Cost-effective policy incentives to achieve an optimal energy mix to reduce the nuclear power in Japan are investigated in [20] through a recursive computable general equilibrium model which uses renewable energy input–output table as an analysis tool. In [21] a system dynamics model along with a game theory model has been presented to find the optimal mix of electricity generation in Iran's electricity industry. The paper [22] proposes a constrained fuzzy multi-objective optimization model to obtain the optimal generation mix of four kinds of renewable power for China's electricity system. Linear programming optimization technique is applied in [23] for optimal development of the renewable electricity generation mix in Spain. In [24], based on the capacity expansion and operations model ETEM (Energy Technology Environment Model), an optimal transition for the Chilean electricity system towards a zero-emissions goal is computed.

A multi-region ESOMs which exploit complementarity between different energy sources in different regions are given in [15,26,56–65]. A review of spatial resolution and regionalization in national-scale ESOMs is given in [66]. Large number of decarbonization scenarios for the United States are investigated in [15] using the GenX model [34] formulated as mixed integer linear programming problem. The geographic differences in renewable resource potential and patterns of demand are accounted for using data from two dissimilar regions of the United States. A linear least-cost dispatch and investment model is applied in [26] to investigate 100% renewable energy (RE) scenarios for North America using the AnyMOD framework [67] with spatially disaggregated data on renewable resources in a high temporal resolution. Differential evolution is used to find the optimal generation structure for complete decarbonization of electricity generation in Japan [56] and Australia [57]. The multi-objective model for planning 100% RES scenarios, maximizing the complementarity between hydro, wind and PV resources and minimizing the total expansion costs is developed in [58] and demonstrated on the example of Brazilian power system. Different Pareto optimal points were generated by applying the hierarchical method and solving the defined problem by sequential quadratic programming algorithm. In [59], a linear optimization was used to explore zero-carbon electricity systems for the US, co-optimizing regional capacity investments and hourly operation of generation, storage, and transmission investment (both within regional and inter-regional) to meet projected electricity demand in 2040. In [60], 100% RE systems for the Middle East and North Africa region are investigated utilizing the LUT Energy System model [68] that works based on a linear optimization algorithm. In [61], the energy system model for the Bolivian power system takes into account the systems flexibility by modelling unit commitment. This model is solved by mixed integer linear programming. In contrast to papers [56–61], paper [62] proposes the optimal energy mix for a Southeast Asian region which minimizes the risk caused due to future uncertainties related to energy demand, volatile fuel price and evolution of renewable technologies using stochastic optimization. An optimal energy resource mix for the US and China to meet emissions pledges was investigated in [63] using the combined energy and geoengineering optimization model [64] which incorporates specific code to account for the effects of tree planting as a means of carbon sequestration and also the cost of the tree planting. The welfare maximizing energy mix within Europe was analyzed in [65] by a dynamic optimal growth general equilibrium model.

Both single-regional and multi-regional ESOMs often do not consider intra-regional RES variability, as stated in [69]. These regions are usually determined based on the administrative boundary not on RE resource potential. Modelling of intra-regional RES variability enables us to exploit the complementarity of RES to larger extent than energy models which employ lower spatial resolution. The effect of more detailed representation of the spatial distribution of RE potential on the results of ESOMs is investigated in [70]. The temporal resolution used in ESOMs is often small; hence, it does not simulate the realistic flexibility requirements of the power system. Intra-regional RES variability is modelled in [56–58], [71–73] with high temporal resolution. Although the concept of complementarity is often not directly discussed, complementarity of renewable resources is implicitly used in the optimization of energy systems when RES are modelled as spatially distributed [74]. Supply side complementarity for different locations around the world is investigated in [11] without considering the complementarity with the local demand profiles, although it was recognized as an important aspect. Paper [11] used the stability coefficient defined in [12] to describe hybrid mixes of complementary variable RES. In paper [12] it was discussed that hybrid mixes of variable RES could be 'tuned' to better match the local demand profile before calculating their stability index.

In this paper, we propose an approach to long-term RES development for the scenario of complete decarbonization of electric energy generation in an electrical energy independent power system. An optimization model for the structure and spatial allocation of installed capacities of wind and PVPPs developed in this paper will give solution for which the best possible adjustment between the total RES generation profile and the referent consumption profile while satisfying the optimization constraints. This approach uses the physical flows of energy as the foundation for long-term planning, which is good because they are independent of economic, political and social factors, in contrast to the previously mentioned papers. This way the uncertainty related to the assumptions of future primary fuel and technology costs is avoided. The referent consumption profile was defined as the part of the total electricity consumption profile which is supposed to be supplied as much as possible directly from variable RES. The measure of the adjustment between these profiles is the sum of squared errors where an error is defined as the difference between the total RES generation and the referent consumption in an hour. The optimization constraints bound the installed power plant capacity in each region according to the estimated technically available potential for the construction of WPPs and PVPPs and force the total energy production to equal the targeted energy needs. This model uses the natural complementarity that exists between generation profiles of wind and PVPPs in different regions to minimize the sum of squared errors. By using the least squares (LS) method, our approach shapes the difference between the RES generation and the referent consumption profile (the imbalance profile). This imbalance profile taken with negative sign represents the total generation profile of all the other participants in maintaining the demand-supply balance in the considered power system (dispatchable power plants, flexible power plants, storage systems, demand side management). This method makes a compromise between minimizing the total energy surplus in the system that the balancing capacities need to accommodate, minimizing the total energy deficit in the system that the balancing capacities need to supply and minimizing the magnitude of the maximal imbalance power which defines the necessary installed power of the balancing capacities. To the best of the authors' knowledge, this approach to alleviating the power system flexibility requirements has not been applied elsewhere. The optimization model uses multi-year hourly profiles, and this way captures the mutual correlations between generation profiles of different energy sources and the total gross consumption profile, as well as annual climate variations. The electric power system in concern can surpass the boundaries of a state and comprise several states, i.e., an electric energy independent region can be planned using this approach.

In Section 2, we describe the proposed approach to long-term RES development planning. The mathematical model for optimizing the structure and spatial allocation of utility scale wind and PVPPs is given in Section 3. In Section 4, the application of the proposed methodology on the Serbian power system is described and the analysis of the obtained results is given. The conclusions are stated in Section 5.

## 2. The Proposed Approach to Long-Term Planning of Renewable Energy Sources Development for the Scenario of Complete Decarbonization of Electric Energy Generation

The analysis of the available wind and PV resource on the territory of the analyzed electric power system is performed first in order to identify regions with technically usable wind and PV energy potential. By consulting the orographic maps and taking into account the available road and power system infrastructure, as well the required distance from populated areas, the available surface area for constructing WPPs and utility scale PVPPs is estimated for each of the identified regions and their maximal acceptable installed capacity.

In certain time periods, characteristics of wind and PV resource in different regions differ from each other regarding the capacity factor and the shape of the hourly profile wind and PVPP specific electric energy generation (electric energy generation profile of the unit capacity power plant). This means that the certain amount energy, which should be obtained from RES in the future power system, could be produced from RES with different structure and spatial allocation of the installed capacity of WPPs and PVPPs into the identified regions. By using the complementarity between hourly profiles of specific generation of WPPs and PVPPs in different regions, which exists both on the daily and seasonal level, it is possible to determine the structure and spatial allocation of the wind and PV installed capacities so that the total RES generation profile is optimally adjusted with the referent consumption profile under the condition that the total amount of energy generated from RES satisfies the specified energy demand. These RES capacities must satisfy the constraints imposed by the available surface area for their construction in certain regions. Additionally, it has to be taken into account that the existing RES capacities in the power system will contribute to supplying the referent consumption profile. For the criterion describing the adjustment between the total RES generation profile and the referent consumption profile, we used the sum of squared differences between coincident hourly values of these profiles. The lesser value of this criterion means better adjustment between the profiles.

Besides the WPPs and utility scale PVPPs, it is necessary to plan the development of the distributed PV systems at the same time. Distributed PV systems are installed in load centers on the roofs of buildings or on the ground structures. The maximal distributed PV capacity connected in a distribution network can be constrained by the available surface area for their mounting, but also with the network hosting capacity. By suitable planning of the distributed PV penetration level the beneficial effect regarding distribution network energy losses reduction can be achieved. In order to ensure even development of distributed PV systems in all load zones and distribution network energy losses reduction, we set the condition that the installed capacity of distributed PV systems in each distribution network must result in the same level of Joule's losses reduction. For the calculation of capacities of distributed PV systems, the active and reactive consumption power profiles as well as the specific generation profiles of distributed PV systems must be known for each distribution network. Therefore, when planning the development of WPPs and utility scale PVPPs, it is necessary to define first which scenario for the development of the distributed PV systems is assumed, i.e., how much of the distributed PV systems capacity is supposed to be installed in each distribution network.

As described above, the proposed methodology requires preparation of the hourly profiles of the specific electric energy generation for each of the identified regions which fulfill the technical requirements for the construction of WPPs and PVPPs. Besides preparing these profiles, one of the key tasks of the proposed methodology is the determination of the referent consumption profile. We define the referent consumption profile as the difference between the future gross consumption profile in the analyzed power system and the sum of the planning profiles of dispatchable power plants (which can be non-fossil fuel TPPs or nuclear power plants) and the representative generation profiles of run-of-the-river and accumulation hydro power plants (HPPs). The representative generation profiles are based on data from several successive years which represent well the climatic conditions in the analyzed territory. These years define the referent time period for the long-term planning of RES. The specific generation profiles of WPPs and PVPPs have to also be defined for the referent time period in order to capture the mutual correlations between generation profiles of different energy sources in the system and the consumption profile. The planning profile of a nuclear power plant is defined as the profile of constant power which equals the rated power of the nuclear power plant. Non-fossil fuel TPPs in future power systems are planned for cogeneration and to provide this way the thermal energy supply of those loads which are in the actual power system supplied from cogeneration fossil-fuel TPPs. For the definition of this planning profile, the thermal energy profile generated from fossil-fuel TPPs in the actual power system during the referent time period has to be known. The planning profile of an accumulation HPP for a referent year is formed in the following way: the total energy generated from this power plant is distributed in time proportionally to the monthly average inflow into its reservoir. The planning profile of a run-of-the-river HPP for a referent year has to take into account the discharge of water from the upstream accumulation HPPs, if such exists. The time this discharge travels from the upstream HPP can be neglected if it is less than 24 h. If the run-of-the-river HPP has the capability of accumulating water during one day, then its planning profile is defined as the generation profile corresponding to the natural inflow which is averaged on a daily basis. This profile is determined using the representative generation curve for the considered run-of-the-river HPP. The representative generation curve is defined as the polynomial curve which approximates best the historical data about daily average generated energy corresponding to certain daily average discharge of the run-of-the-river HPP. If the considered run-of-the-river HPP does not have a significant capability for accumulating water, its planning profile is defined as the historical hourly generation profile realized in the referent time period.

In most power systems, capacities for HPPs development are mostly exhausted. In power systems which have the potential for the construction of additional HPPs, it is assumed that the whole technical capacity will be used in the future and that the allocation of these HPPs is determined. While generation profiles of the existing HPPs are taken into account in the proposed model based on the realized energy generation in the previous period of time, for the HPPs planned to be constructed in the future, generation profiles are estimated based on the natural river flows on the locations planned for the HPPs development and the estimated rated power of these HPPs.

The proposed planning methodology is illustrated in Figure 1. The proposed algorithm requires the following input data for the analyzed power system:

1. The hourly profile of the total power consumption for the referent time period;
2. The hourly planning profiles of the conventional non-fossil dispatchable power plants for the referenced time period. An example for the calculation of this profile for biogas power plants is given in Section 4.2.5.
3. The hourly representative generation profiles of the existing and planned run-of-the-river and accumulation HPPs for the referent time period. An example for the calculation of these profiles is given in Section 4.2.4.
4. The hourly generation profiles of the existing and planned distributed PV systems for the referent time period. The model for calculating this set of input data and a calculation example are given in Section 4.2.3.
5. The maximal acceptable installed capacity and hourly specific generation profiles (MWh/MW/h) of the existing and planned utility scale PVPPs for each of the identified regions for the referent time period. The model for calculating this set of input data and a calculation example are given in Section 4.2.2.
6. The maximal acceptable installed capacity and hourly specific generation profiles (MWh/MW/h) of the existing and planned WPPs for each of the identified regions for the referent time period. The model for calculating this set of input data and a calculation example are given in Section 4.2.1.

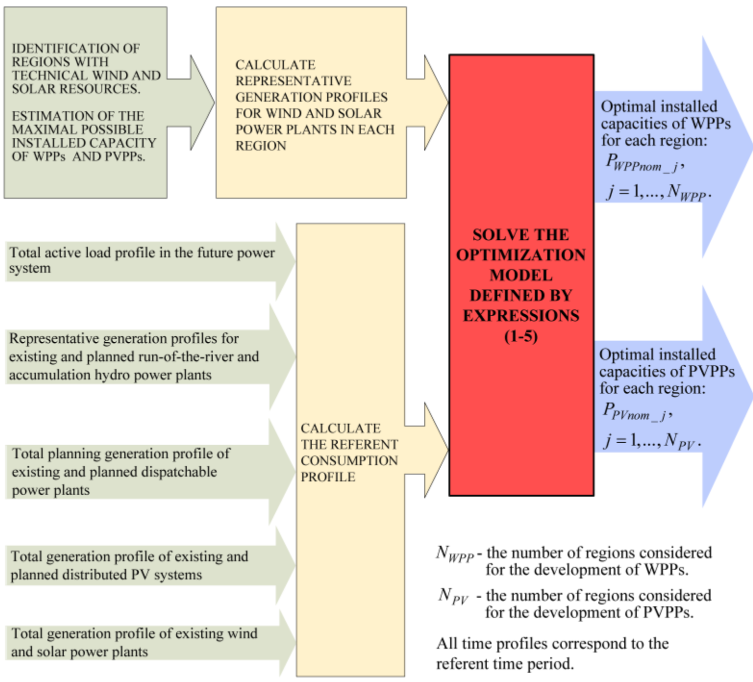


**Figure 1.** The proposed algorithm for planning RES development for complete decarbonization of electrical energy generation.

The referent time period consists of the whole number of years. It is preferable for the referent time period to cover several years in order to capture the variation of the RES potential and the consumption profile weather dependency over the years.

The outputs of the proposed algorithm are:

1. The optimal installed capacity of utility scale PVPPs for each of the identified regions;
2. The optimal installed capacity of WPPs for each of the identified regions.

Tables 1 and 2 show the output data for the analyzed example of decarbonizing the electric energy generation in Serbia according to the proposed methodology. The mathematical model for optimizing the structure and spatial allocation of RES is described in the following section.

## 3. The Mathematical Model for Optimizing Structure and Spatial Allocation of RES for the Scenario of Complete Decarbonization of Electrical Energy Generation

The mathematical model for optimizing structure and spatial allocation of RES for the scenario of complete decarbonization of electrical energy generation is defined as a linear LS problem with linear constraints. Since the problem is constrained, the usual methods used for solving the unconstrained LS problem, i.e., for solving the normal equations, cannot be applied. Our problem is large-scale. The number of rows of the system matrix is in the range of tens of thousands and the number of columns is in the range of several tens. Namely, the system matrix $A$ is defined as:

$$A = \begin{bmatrix} P_{WPPspec\_1}(t_1) & \dots & P_{WPPspec\_N_{WPP}}(t_1) & P_{PVspec\_1}(t_1) & \dots & P_{PVspec\_N_{PV}}(t_1) \\ P_{WPPspec\_1}(t_2) & \dots & P_{WPPspec\_N_{WPP}}(t_2) & P_{PVspec\_1}(t_2) & \dots & P_{PVspec\_N_{PV}}(t_2) \\ \vdots & & \vdots & \vdots & & \vdots \\ P_{WPPspec\_1}(t_{N_h}) & \dots & P_{WPPspec\_N_{WPP}}(t_{N_h}) & P_{PVspec\_1}(t_{N_h}) & \dots & P_{PVspec\_N_{PV}}(t_{N_h}) \end{bmatrix}, \tag{1}$$

where $P_{WPPspec\_j}(t_k), j = 1, \dots, N_{WPP}$, an $P_{PVspec\_i}(t_k), i = 1, \dots, N_{PV}$, designate the specific generation of WPPs and PVPPs in region $j$ in the $k^{th}$ hour of the referent planning period, $k = 1, \dots, N_h$. The referent planning period consists of $N$ years. The number of regions with technically exploitable wind and PV potential is $N_{WPP}$ and $N_{PV}$, respectively.

In general case matrix $A$ could be singular or nearly singular. The most reliable methods for solving such large-scale LS problems are based on transforming the system matrix in some of the canonical forms using orthogonal transformations. This way the exacerbation of problem conditioning is avoided. The complexity of solving a LS problem depends on the rank of the system matrix. In general case, the system matrix in our problem could be rank-deficient, also linear constraints could be linearly dependent, so the solving algorithm needs to take care of such cases. We applied the following approach to our problem. The linear LS problem with linear constraints is first transformed into the equivalent least-distance problem [75,76] using the matrix singular value decomposition and applying the appropriate strategy for estimating the numerical rank of matrices. This provides the numeric stability of the calculation. Then, the dual approach is applied, which was used also Lawson and Hanson [77], Cline [76], Haskell and Hanson [78], and the problem is solved by applying the LDP (Least Distance Programming) [77] and NNLS (Nonnegative Least Squares) [77] algorithms as the main tools. These algorithms always converge. The solution to this problem always exists, and in general case there can be infinite number of solutions (when the matrix $A$ is rank-deficient), but even if such situation arises it is possible to determine the unique solution which has minimal Eucledian norm. This solution would also be suitable to our problem because it means that among the solutions we choose the one with the minimal total installed capacity of RES.

The mathematical formulation of the constrained LS model for optimizing structure and spatial allocation of WPPs and utility scale PVPPs is the following:

$$\min_x \|Ax - b\|_2^2 \tag{2a}$$

$$\text{s.t}: \quad x \geq x^{\min}, \tag{2b}$$

$$x \leq x^{\max}, \tag{2c}$$

$$G_m x \geq h^m, m = 1, \ldots, N. \tag{2d}$$

In (2a)–(2d), the coordinates of the decision variables vector $x = \left[x_1 \ldots x_{N_{WPP}+N_{PV}}\right]^{\mathrm{T}}$ are $x_j = P_{WPPnom\_j}, j = 1, \ldots, N_{WPP}$, where $P_{WPPnom\_j}$ is the installed capacity of WPPs in region $j$, and $x_{j+N_{WPP}} = P_{PVnom\_j}, j = 1, \ldots, N_{PV}$, where $P_{PVnom\_j}$ is the installed capacity of PVPPs in region $j$. The vector $x^{\min}$ in (2b) contains the capacities of already existing WPPs and PVPPs in the analyzed regions. The vector $x^{\max}$ in (2c) contains the estimated values of maximal acceptable installed capacities in the analyzed regions. Coordinates of the vector $b = \left[b_1 \ldots b_{N_h}\right]^{\mathrm{T}}$ in (2a) are:

$$b_k = P_{ref\_load}(t_k) - P_{distPVtot}(t_k), k = 1, \ldots, N_h, \tag{3}$$

where $P_{ref\_load}(t_k)$ and $P_{distPVtot}(t_k)$ are, respectively, the referent consumption power and the total distributed PV generation power in the $k^{th}$ hour. Constraint (2d) means that in each year of the referent period the total generated energy in the power system must not be less than the total consumption energy. Matrix $G_m$ and vector $h^m$ are defined as follows:

$$G_m \triangleq \left[g_{ij}{}^m\right]_{1\times(N_{WPP}+N_{PV})}, \; g_{ij}{}^m = \sum_{k=1}^{N_h{}^m} a_{kj}{}^m, \; j = 1, \ldots, N_{WPP} + N_{PV}; \; m = 1, \ldots, N, \tag{4}$$

$$h^m = \sum_{k=1}^{N_h{}^m} b_k{}^m, \; m = 1, \ldots, N, \tag{5}$$

where $N_h{}^m$ denotes the number of hours in the $m^{th}$ year.

Based on the developed mathematical model (1)–(5) and the algorithm shown in Figure 1, it is possible to create software for processing the input data, constrained LS optimization and presenting the results. The proposed algorithm does not require utilization of different solvers integrated in different software tools. The results presented in this paper are obtained using MATLAB software [79] in which m-scripts for data processing and solving the given mathematical model are programmed.

One of the advantages of the proposed solution method is that it is an exact method which guarantees to find the minimum, in contrast to heuristic optimization methods such as the genetic algorithm and similar evolutionary methods. Additionally, the proposed solution method is applicable to large scale problems which often restrain the applicability of other methods. The time needed for code execution depends on the dimensionality of the problem. In the example given in Section 4, the system matrix has 26,280 rows and 26 columns. The problem is solved on Intel® Core™ i5-10210U processor with 8 GB RAM. The wall-clock time needed to solve this problem was about 40 s. The CPU time is about 92 s. The solution method is based on NNLS algorithm which is iterative. The NNLS algorithm performed 20 iterations.

## 4. Demonstration of the Proposed Methodology on the Example of the Power System of Serbia

The application of the proposed methodology is demonstrated on the example of the power system of Serbia. The Serbian power system is undergoing an energy transition towards more sustainable electrical energy generation. Therefore, analysis such as this is necessary in order to strategically plan the decarbonization process. Based on the available national resources, we consider the future generation portfolio consisting of hydroelectric, wind, PV and biogas power plants.

### *4.1. Current Electric Energy Generation Structure in Serbia*

The electrical energy generation in Serbia is dominantly based on lignite fuel TPPs and HPPs (Figure 2a). The annual electrical energy generation from lignite fueled TPPs is in the range of 21–25 TWh, which is around 60–70% of the total electric energy generation in Serbia. Hydroelectric power plants generate in the range of 9–12 TWh annually [80]. Wind power plants generate around 1 TWh annually, whereas the generation of PVPPs was just 10.5 GWh in 2021. Combined heat and power (CHP) and biogas power plants (BPPs) generated around 1.4 TWh of electric energy in 2021 [80]. Figure 2b shows the electrical energy generation structure in Serbia for the period 2017–2019. The total gross consumption of electrical energy in Serbia was 35.479 TWh in 2021. In winter season national electric generation capacities cannot fulfill the consumption demand so the import of electric energy is necessary. In summer season, the consumption is significantly smaller than in the winter season and electric energy is often exported from the Serbian power system.

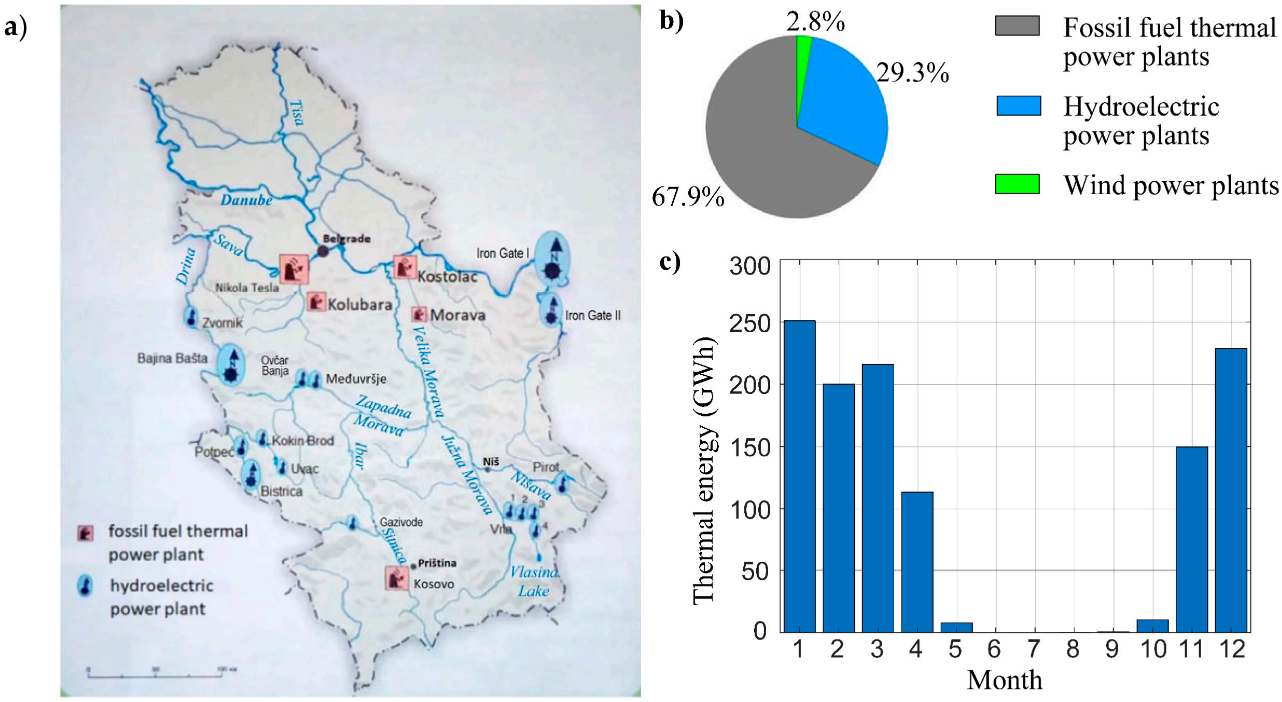


**Figure 2.** (**a**) Electric power plants in Serbia; (**b**) electrical energy generation structure in Serbia; (**c**) thermal energy produced in cogeneration power plants in Serbia.

The actual electrical energy generation structure of the Serbian power system is not long-term sustainable. Besides the problem of carbon emissions causing the greenhouse effect, electric energy generation in Serbia directly relates to the problems of local air pollution which is pronounced in many places in Serbia. According to [81], around 91% of total sulfur oxides and around 42% of total nitrogen oxides in Serbia are caused by electrical energy generation. The average age of TPPs in Serbia is over 40 years and they cannot provide an efficient lignite combustion. Besides the coal combustion related ecological problems, the decarbonization of electric energy generation is inevitable also due to the exhaustion of Serbian coal reserves, which has already affected the operation of thermal units. They often cannot operate with rated power and require oil fuel as a supplement to maintain the combustion stability, which causes additional ecological and economic consequences.

For the reasons given above, it is necessary to implement the decarbonization of electric energy generation in Serbia. Certainly, this process cannot be abrupt, but thermal power plants have to be gradually phased out and replaced by RES accompanied with the appropriate development of balancing capacities which would provide the power system stability.

*4.2. The Energy Potential and Referent Time Profiles of Renewable Energy Generating Capacities for Decarbonizing the Electrical Energy Generation in Serbia*

The procedure for creating generation profiles and estimating maximal capacities of WPPs and PVPPs that can be constructed in regions in Serbia is described in this section.

4.2.1. Identifying the Available Capacities and Specific Electric Energy Generation Profiles from WPPs

Based on the available map of wind energy potential of Serbia, the available wind parameters measurement data, orographic characteristics of the terrain, road and electric power system infrastructure and the restrictions imposed by nature conservation areas, the regions with potential for WPPs development are identified. Wind parameters measurement data for 21 locations in the identified windy regions in Serbia (shown in Figure 3) are obtained either from dedicated measuring masts or from virtual masts. Virtual measurement data cover a one-year period with hourly resolution of the wind speed, wind direction and air density on measuring heights of 100 m, 120 m and 140 m. These data are obtained from Vortex database using ERA 5 global meteorology database.

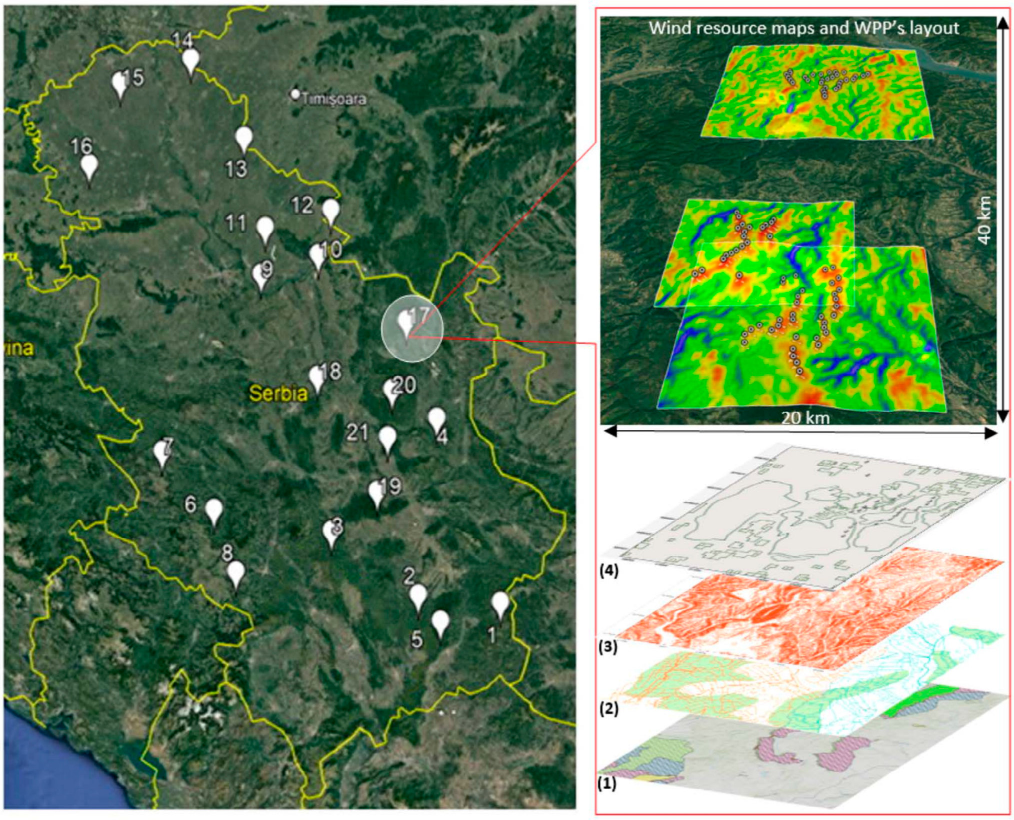


**Figure 3.** Positions of the measuring points in the identified windy regions in Serbia (denoted by numbers 1–21) with the illustration of the wind energy potential estimation for a single target region. Layers: (1) Nature protected areas, (2) Urbanism and infrastructure, (3) Orography, (4) Roughness.

For each of the identified regions with good wind energy potential, an analysis of conditions and constraints regarding the development of WPPs' projects was conducted comprising several steps, i.e., layers defining the constraints:

(1) Nature protected areas layer: This layer is formed based on the available maps with nature protection area coverage in Serbia [82]. These areas include the spatial units in which certain protected areas are located, along with the areas defined by international programs for the identification of Important Plant Areas (IPA), Important Bird Areas

(IBA), Prime Butterfly Areas (PBA), Ramsar areas, Emerald Areas, etc. These areas are excluded from consideration for possible WPPs construction.

(2) Urbanism and infrastructure layer: This layer is formed based on the available data from national geoportal of Serbia [83], as well as the other available data regarding the road and electric power system infrastructure. Based on the available infrastructure, the conveniences and constraints for the construction of WPPs are considered, also the necessary distance of these plants from the populated locations, roads and power lines was defined. Inaccessible areas for which it was estimated that the construction of road and power system infrastructure would be too expensive, were set apart.

(3) Orography layer: For creating the wind potential map and planning the WPP layout, it is necessary to prepare the orography map of the terrain. The vector map of the terrain orography was created using the WAsP software based on the data obtained from the SRTM (Shuttle Radar Topography Mission) database [84].

(4) Roughness layer: For creating the wind potential map, it is necessary to prepare the terrain roughness maps first. This map is created in the WAsP software based on the Corine land data obtained from the Copernicus Land Monitoring Service [85] and orthophotos of the terrain obtained from [83].

By using the described layers, the available space for the construction of WPPs is estimated for each of the identified regions and the high-resolution maps $(100\text{ m} \times 100\text{ m})$ of wind energy potential are created using the WAsP software [86]. The wind class is determined for each region, the reference wind turbine is chosen, and spatial positioning of wind turbines is determined. This way the maximal capacity for installing WPPs is estimated for each region. Figure 3 illustrates the described approach on the example of region 17 for which the maximal installed capacity of 600 MW is estimated. The estimated maximal WPPs' capacities are given in the fourth column of Table 1 for each of the identified regions.

Specific generation profile of WPPs is for region $j$ calculated in the following way. First, the expected annual energy generation, $W_{WAsP\_j}$, for the representative wind turbine (the wind turbine with average annual electricity production of the WPPs in the analyzed region) is calculated using the WAsP software. Then, the hourly generation profile of the representative wind turbine is calculated based on the wind turbine power curve and the available wind speed data. The wind speed, $V_{ji}$, and air density, $\rho_{ji}$, measured at the representative wind turbine mast height in the $i^{th}$ hour in the $j^{th}$ region are used to calculate the effective wind speed, $V_{eff\_j}(t_i)$, according to the following expression:

$$V_{eff\_j}(t_i) = V_{ji}\left(\frac{\rho_{ji}}{\rho_0}\right)^{\frac{1}{3}}, \tag{6}$$

where $\rho_0 = 1.225\,\text{kg}/\text{m}^3$ is the standard air density for which the wind turbine power curve is defined.

Based on the power curve of the chosen wind turbine and the calculated net annual generation the following equation is defined:

$$\sum_{i=1}^{8760} \Delta t \cdot P_{power\_curve\_j}(\eta_j V_{eff\_j}(t_i)) = W_{WAsPj}, \Delta t = 1\text{ h}, j = 1, \ldots, 21. \tag{7}$$

The scaling coefficient for region $j$,$\eta_j$, takes into account corrections due to spatial and height extrapolation of wind speed within the analyzed region, losses due to wake effect and other losses in a WPP. It is determined from (7) through an iterative procedure. After that, the hourly specific generation of WPPs, $P_{WPPspec\_j}(t_i)(\text{MW}/\text{MW}_{\text{rated}})$, is calculated for each region $j$ :

$$P_{WPPspec\_j}(t_i) = \frac{P_{power\_curve\_j}\left(\eta_j V_{eff\_j}(t_i)\right)}{P_{WPPnom\_j}}, j = 1, 2, \ldots 21; i = 1, 2, \ldots 8760, \tag{8}$$

where $P_{WPPnom\_j}$ is the rated power of the representative wind turbine for region $j$.

#### 4.2.2. Identifying the Available Capacities and Specific Electrical Energy Generation Profiles from Utility Scale PVPPs

In order to identify suitable locations for the development of utility-scale PVPPs, the territory of Serbia is considered through 5 regions (Table 2) which are defined by grouping certain administrative districts shown on the left in Figure 4. Each region is investigated for the suitable locations for utility scale PVPPs construction. With regard to solar potential, its spatial dispersity is not particularly prominent, therefore, the PVPPs' development can be considered practically on all locations which satisfy space and urbanistic requirements. The identifying of the locations and estimation of the PV energy potential is conducted through several steps, i.e., layers which define different constraints regarding the development of the utility-scale PVPPs:

(1) Nature protected areas layer: This layer is formed based on the available maps of protected areas in Serbia. These areas were excluded from the consideration of PVPPs' development.
(2) Soil quality layer: PVPPs require the occupation of large areas, which is their main disadvantage. To reduce this negative effect, their development should be planned on devastated land (tailing ponds in open pit mines, ash ponds of coal-fired thermal power plants) and low-quality agricultural land (low quality grassland and thickets). The soil quality layer is created based on data from [84,87].
(3) Urbanism and infrastructure layer: This layer contains data about land ownership, land category and the road and electric power system infrastructure. Conveniences and constraints for the development of PVPPs regarding the available infrastructure are considered. In general, PVPPs are planned on large parcels near the road and electric power system infrastructure.
(4) Topography layer: Terrain topography is analyzed using the maps created based on the data from [85] and Google Earth satellite images of the terrain. The development of PVPPs today is mostly based on two concepts: systems with horizontal single-axis solar trackers which provide following the azimuth angle of the Sun and systems with fixed constructions and suitably oriented modules. Systems with solar trackers require even surface with inclination less than 15° while fixed constructions can be mounted even on terrains with more complex topography. Both systems require relatively large surface areas. The usual surface area requirement is $1 - 1.3\,\mathrm{ha/MWp}$ (larger values for systems for solar tracker than for fixed systems). Based on the topography layer, locations with suitable inclination and surface orientation are chosen and the possibility for the development of PV systems with single-axis trackers is considered.

The described approach to capacity estimation for PVPPs' development in the region of Eastern Serbia is illustrated in Figure 4. On the designated area in Figure 4, it is possible to build 650 MWp in total. A similar procedure is applied to estimate maximal PVPPs' capacity in other locations in all 5 regions. These capacities are shown in the fourth column of Table 2.

Multi-year hourly profiles of specific PV electric generation (MWh/MWp/h) are calculated for each of the specified regions using PVGIS software and SARAH2 database [88]. Since the PVPPs efficiency decreases during the exploitation period, when calculating their specific generation profiles, it was assumed the PV module efficiency which corresponds to the middle of the exploitation period. The exploitation period is assumed to be 25 years and the average annual efficiency degradation of PV modules due to age is assumed to be 0.5% from the declared efficiency for new PV modules. This approach could be justified by the following consideration. Since the process of decarbonization and the development of PVPPs in distribution and transmission networks is a long-term process, the installed PVPPs will consist of the newly installed and of the ones which are near the end of lifetime. Therefore, it can be assumed that in the completely decarbonized power system PVPPs will, on average, operate with the efficiency corresponding to the middle of their lifetime.

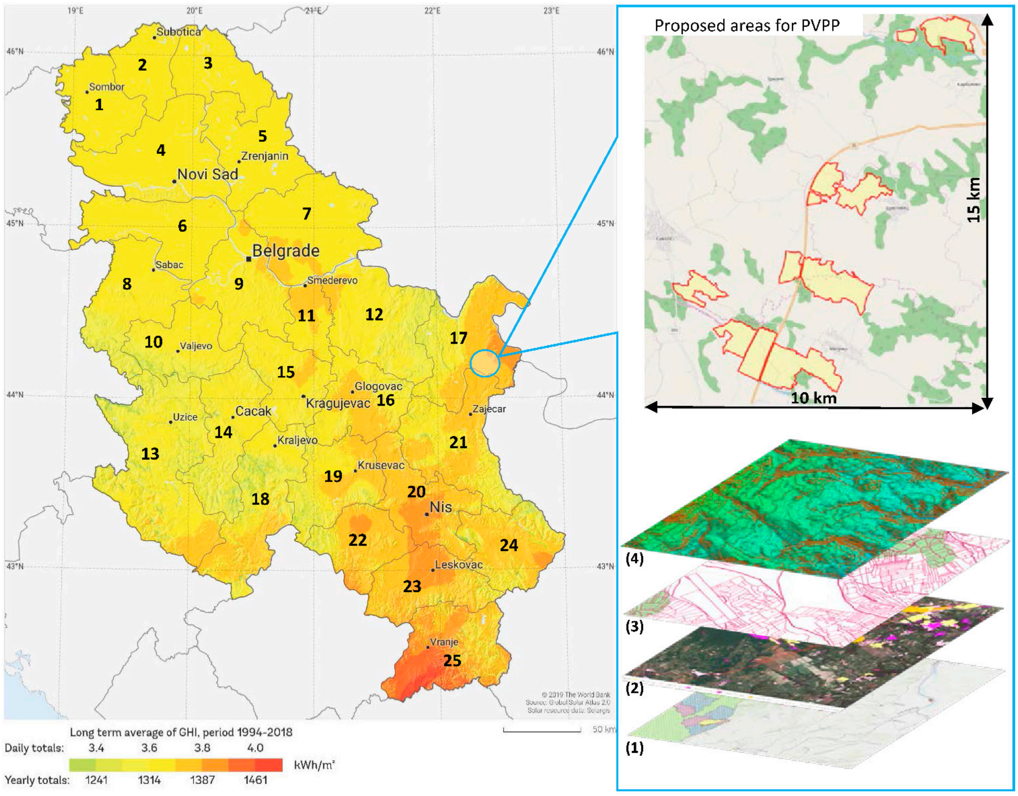


**Figure 4.** The map of global horizontal irradiation [89] in the Republic of Serbia with the illustration of PV energy potential estimation for a single targeted region. The numbers 1–25 denote the administrative districts in Serbia. Layers: (1) Nature protected areas, (2) Soil quality, (2) Urbanism and infrastructure, (4) Topography.

#### 4.2.3. Analysis of Capacities and Specific Profiles for Electric Energy Generation from Distributed PV Systems

The distributed PV systems are planned to be developed in all distribution networks in such a way as to achieve approximately the same relative reduction in distribution network losses. The distribution networks considered are the ones supplied from exactly one electrical point, i.e., a transformation station 110/X kV/kV. The number of distribution networks is designated as $N_{dist}$. The hourly profiles of active and reactive power measured on the high voltage side of each transformation station 110/X kV/kV in the power system of Serbia are used for calculating the distributed PV systems' capacities. The specific PV generation profiles, $P_{distPV\_i}{}^{spec}$, for each distribution network are obtained from PVGIS SARAH2 database [88]. These profiles are scaled to take into account the PV module efficiency degradation in the middle of their 25-year lifetime, as it was adopted for utility scale PVPPs. The model for planning distributed PV capacities in order to achieve the requested level of Joule's losses reduction is described in the following.

If capacity $x_{dist\_i}$ of distributed PV systems is installed in the $i^{th}$ distribution network, then the effect on total Joule's losses is this network can be described by the following expression which defines the relative reduction in Joule's losses in that network, $y_{J\_i}$ :

$$y_{J\_i} = \left( 1 - \frac{\frac{R_{eq\_i}}{U_{n\_i}} \sum_{k=1}^{N_h} \left[ \left( P_{load\_i}(t_k) - P_{distPV\_i}{}^{spec}(t_k) x_{dist\_i} \right)^2 + Q_{load\_i}(t_k)^2 \right]}{\frac{R_{eq\_i}}{U_{n\_i}} \sum_{k=1}^{N_h} \left( P_{load\_i}(t_k)^2 + Q_{load\_i}(t_k)^2 \right)} \right) \cdot 100 = c_{2i} x_{dist\_i}{}^2 + c_{1i} x_{dist\_i}, i = 1, \ldots, N_{dist}, \quad (9)$$

where $R_{eq\_i}$ is the equivalent resistance which models the total Joule's losses in the $i^{th}$ distribution network, $P_{load\_i}(t_k)$ and $Q_{load\_i}(t_k)$ are, respectively, the active and reactive power measured at the high voltage side of the transformation station 110/X kV/kV which supplies the $i^{th}$ distribution network in the $k^{th}$ hour. The RMS voltage in this point is assumed to be constant and equal to the rated voltage value, $U_{n\_i}$. Expression (9) neglects the dependency of the equivalent resistance on temperature and distribution network load. Coefficients $c_{2i}$ and $c_{1i}$ are defined as:

$$c_{2i} \triangleq -\frac{100 \cdot \sum_{k=1}^{N_h} P_{distPV\_i}{}^{spec}(t_k)^2}{\sum_{k=1}^{N_h} \left(P_{load\_i}(t_k)^2 + Q_{load\_i}(t_k)^2\right)}, \; i = 1, \ldots, N_{dist}, \tag{10}$$

$$c_{1i} \triangleq \frac{200 \cdot \sum_{k=1}^{N_h} \left(P_{distPV\_i}{}^{spec}(t_k) P_{load\_i}(t_k)\right)}{\sum_{k=1}^{N_h} \left(P_{load\_i}(t_k)^2 + Q_{load\_i}(t_k)^2\right)}, \; i = 1, \ldots, N_{dist}, \tag{11}$$

To achieve the requested value of Joule's losses relative reduction, $y_{J\_i}$, the following distributed PV capacity is required to be installed in the $i^{th}$ distribution network:

$$x_{dist\_i} = \frac{2y_{J\_i}}{c_{1i} + \sqrt{c_{1i}{}^2 + 4c_{2i}y_{J\_i}}}, \; i = 1, \ldots, N_{dist}. \tag{12}$$

For the $i^{th}$ distribution network, the maximal value of Joule's losses relative reduction, $y_{J\_i}{}^{\max}$, is obtained when $x_{dist\_i} = x_{dist\_i}{}^{opt} = -\frac{c_{1i}}{2c_{2i}}$.

Under the condition that the installation of distributed PV systems should in all distribution networks result in approximately the same value of Joule's losses relative reduction, which is as much as possible close to the value $y_J{}^{target}$, the required distributed PV capacities are calculated. If for a certain value of $y_J{}^{target}$ and distribution network $i$ happens to be $y_J{}^{target} > y_{J\_i}{}^{\max}$, then the PV capacity planned for that distribution network will be $x_{dist\_i}{}^{planned} = x_{dist\_i}{}^{opt}$, otherwise, it will be:

$$x_{dist\_i}{}^{planned} = \frac{2y_{J\_\mathrm{target}}}{c_{1i} + \sqrt{c_{1i}{}^2 + 4c_{2i}y_{J\_\mathrm{target}}}}, i = 1, \ldots, N_{dist}. \tag{13}$$

As not all distribution networks can achieve the value $y_J{}^{target}$, the weighted average value of the achieved Joule's losses reduction, $y_{J\_achieved}{}^{avg}$, is calculated for all distribution networks by applying the weighting coefficients equal to the share of each distribution network consumption in the total consumption of all distribution networks.

Considering different values for $y_J{}^{target}$, the curve on Figure 5 is constructed. This curve shows the dependency between the total installed capacity of distributed PV systems, $P_{distPVnom\_tot}$, and the weighted average of Joules' losses reductions achieved in distribution networks in the Serbian power system.

In the following it is assumed that the total installed capacity of distributed PV systems will equal 1940.7 MW in the future power system of Serbia and that this capacity is allocated to distribution networks using the approach described above.

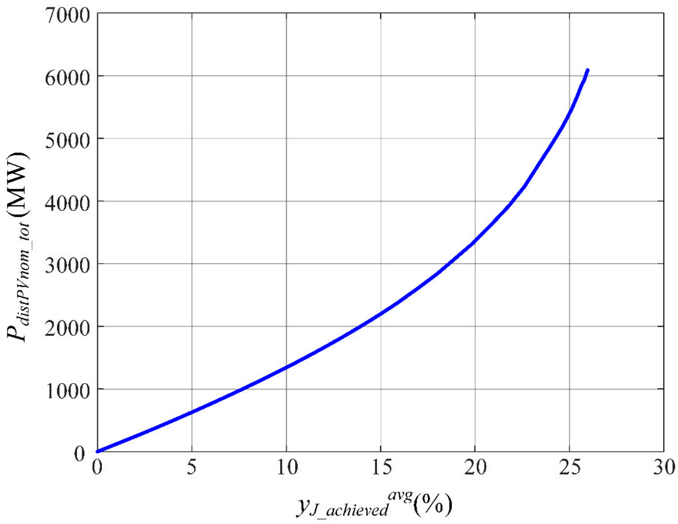


**Figure 5.** The required installed capacity of distributed PV systems for achieving a certain weighted average value of Joule's losses reductions in distribution networks in Serbia.

#### 4.2.4. The Representative Generation Profiles of Hydroelectric Power Plants

There are several accumulation and run-of-the-river HPPs in the Serbian power system. Their locations are shown in Figure 2a. The representative generation profiles for accumulation HPPs "Uvac", "Kokin Brod", "Bistrica", "Pirot", "Vrla 1–4" are formed by distributing the total annual energy generation of the power plants proportionally to the monthly average inflows into the reservoir. Figure 6a shows the profile for HPP "Uvac".

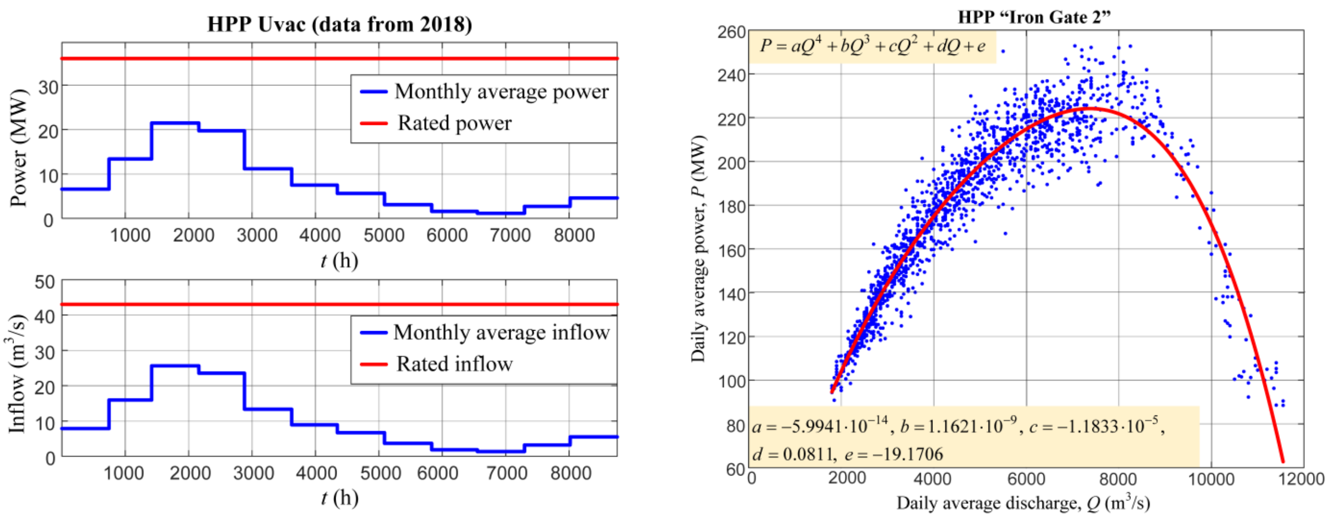


(**a**) (**b**)

**Figure 6.** (**a**) Representative generation profile for HPP "Uvac"; (**b**) representative generation curve for HPP "Iron Gate 2".

The representative generation profiles for run-of-the-river HPPs with the capability of accumulating water within single day: "Iron Gate 1", "Iron Gate 2", "Potpeć", "Zvornik", "Bajina Bašta" are formed using the representative generation curves such as the one in Figure 6b which refers to HPP "Iron Gate 2". Their annual hourly profiles are created from daily average values. For HPPs "Međuvršje" and "Ovčar Banja" historical hourly values of electric energy generation are used. The future installed capacity of HPPs is assumed to remain the same as today.

#### 4.2.5. The Planning Generation Profile of Biogas Power Plants

Future installed capacity of BPPs is planned to provide the same amount of thermal energy generation which is in the present power system supplied from cogeneration plants (Figure 2c). It is assumed that a 1 MW power plant produces electric and thermal energy in the ratio 1:1.0875 and that its self-consumption takes 10% of electric energy and 25% of thermal energy [90]. Knowing the monthly thermal energy generation profile from gas power plants, the necessary total installed capacity of BPPs their monthly average electric power generation profile is calculated. The required total installed capacity of BPPs is 180.5 MW.

### *4.3. The Referent Consumption Profile*

The suggested optimization model for the RES capacity structure and spatial allocation requires the perspective total consumption profile in the Serbian power system to be known. Since the consumption of electric energy in Serbia has not pronounced significant changes in recent years, the optimization is performed under the assumption that the electric energy consumption profile in the future will be the same as in the actual Serbian power system. The reference consumption profile to be used in our optimization model is the difference between the total hourly consumption profile and the sum of planning profiles of BPPs, run-of-the-river HPPs and accumulation HPPs. In order to capture the weather dependency of these profiles and their mutual correlations, the multi-year time period of coincident data should be used. For the power system of Serbia, we considered the period of 2017–2019. The river flows of HPPs were significantly below average in 2017 and significantly above average in 2019.

### *4.4. Results*

The optimal structure and spatial allocation of WPPs and utility scale PVPPs for the scenario of complete decarbonization of electrical energy generation in Serbia is given in Tables 1 and 2. The amount of directly supplied consumption energy is 81.8553 TWh which presents 84.3% of the total consumption energy in the Serbian power system in the considered period (Table 3). Shares of different generation technologies in the total electric energy generation for the future power system of Serbia are shown in Figure 7. Figure 8 shows different generation technology shares in the total generation profile.

**Table 1.** Optimal capacities of WPPs in regions with technically exploitable wind resource.

| Region | Coordinates of the Measuring Point | Lower Limit (MW) | Upper Limit (MW) | Optimal Value (MW) |
|---|---|---|---|---|
| 1. Vlasinski region | 42.630402°, 22.351410° | 0 | 300 | 300.0 |
| 2. Medveđa—Sijerinska banja | 42.744032°, 21.700192° | 0 | 300 | 300.0 |
| 3. Kuršumlija—Kopaonik | 43.166227°, 21.068085° | 0 | 200 | 0.0 |
| 4. Sokobanja—Boljevac | 43.690319°, 22.052176° | 0 | 350 | 350.0 |
| 5. Vranje—Bujanovac | 42.581659°, 21.84849° | 0 | 300 | 300.0 |
| 6. Nova Varoš—Ivanjica | 43.379707°, 20.125107° | 0 | 300 | 2.3 |
| 7. Zlatibor | 43.738277°, 19.747049° | 0 | 200 | 200.0 |
| 8. Tutin—Pešterska visoravan | 43.07063°, 20.29788° | 0.4 | 300 | 300.0 |
| 9. Beograd—Smederevo | 44.636960°, 20.750840° | 0 | 350 | 0.0 |
| 10. Požarevac—Golubac—Kučevo | 44.695554°, 21.252526° | 0 | 1200 | 503.1 |
| 11. Južni Banat—Pančevo | 44.891035°, 20.832648° | 380.96 | 1800 | 1278.8 |
| 12. Južni Banat—Bela Crkva | 44.930052°, 21.405840° | 6.6 | 300 | 6.6 |
| 13. Srednji Banat | 45.412857°, 20.742172° | 0 | 1000 | 0.0 |

**Table 1.** *Cont.*

| Region | Coordinates of the Measuring Point | Lower Limit (MW) | Upper Limit (MW) | Optimal Value (MW) |
|---|---|---|---|---|
| 14. Severni Banat | 45.899215°, 20.354914° | 0 | 600 | 0.0 |
| 15. Severna Bačka | 45.828923°, 19.715525° | 9.9 | 1800 | 1800.0 |
| 16. Južna Bačka | 45.391719°, 19.371972° | 0 | 600 | 98.0 |
| 17. Bor—Majdanpek—Negotin | 44.179440°, 21.94357° | 0 | 600 | 600.0 |
| 18. Kragujevac—Jagodina | 44.023020°, 21.11047° | 0 | 150 | 150.0 |
| 19. Niš—Prokuplje | 43.345336°, 21.48325° | 0 | 300 | 300.0 |
| 20. Paraćin—Boljevac | 43.885314°, 21.71861° | 0 | 100 | 100.0 |
| 21. Aleksinac—Ražanj | 43.632383°, 21.62856° | 0 | 500 | 500.0 |
| **Total:** | | **397.46** | **11,550** | **7088.7** |

**Table 2.** Optimal capacities of utility scale PVPPs in regions with technically exploitable PV resource.

| Region | Coordinates of the Measuring Point | Lower Limit (MW) | Upper Limit (MW) | Optimal Value (MW) |
|---|---|---|---|---|
| 1. Northern Serbia (regions 1–8) | 45.918°, 20.362° | 0 | 1150 | 732.7 |
| 2. Central Serbia (regions 9,10,11,15,16) | 44.399°, 20.400° | 0 | 3500 | 0 |
| 3. Eastern Serbia (regions 12,17,21) | 44.161°, 22.374° | 0 | 1700 | 849.3 |
| 4. Western Serbia (regions 13,14,18,19) | 43.239°, 20.210° | 0 | 800 | 495.3 |
| 5. South Serbia (regions 20,22,23,24,25) | 42.477°, 21.809° | 0 | 1600 | 1036.0 |
| **Total:** | | **0** | **8750** | **3113.4** |

**Table 3.** Characteristics of the consumption covering for the optimized structure and spatial allocation of RES (for the analyzed three-year referent time period). The directly supplied energy is marked red as it is the main result.

| Min. Sum of Squared Errors ($f_{\min} = \|Ax_{opt} - b\|_2^2$) (MWh$^2$) | Total Generated Energy (TWh) | Total Consumed Energy (TWh) | Directly Supplied Energy (TWh) | Total Surplus Energy (TWh) | Total Shortage Energy (TWh) |
|---|---|---|---|---|---|
| $6.5626 \times 10^{10}$ | 99.5953 | 97.0935 | 81.8553 | 17.7400 | 15.2369 |

We call the difference between the total generation profile and the total consumption profile the imbalance power profile. The imbalance power profile is also equal to the error profile in model (1)–(5), which is the difference between the total WPP and utility scale PVPP generation profile and the referent consumption profile. The imbalance power profile which corresponds to the optimal structure and spatial allocation of WPPs and PVPPs in Serbia is shown in Figure 9. Its characteristics are given in Table 4. Figure 10 also shows the imbalance power profile but with indicated periods in which the surplus and shortage of energy occur.

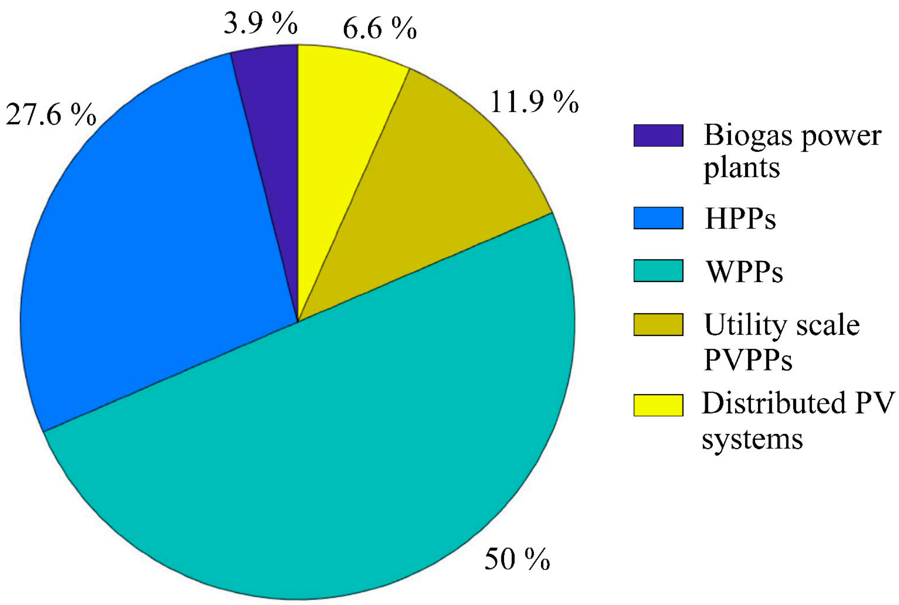


**Figure 7.** Electric energy generation structure in the completely decarbonized Serbian power system.

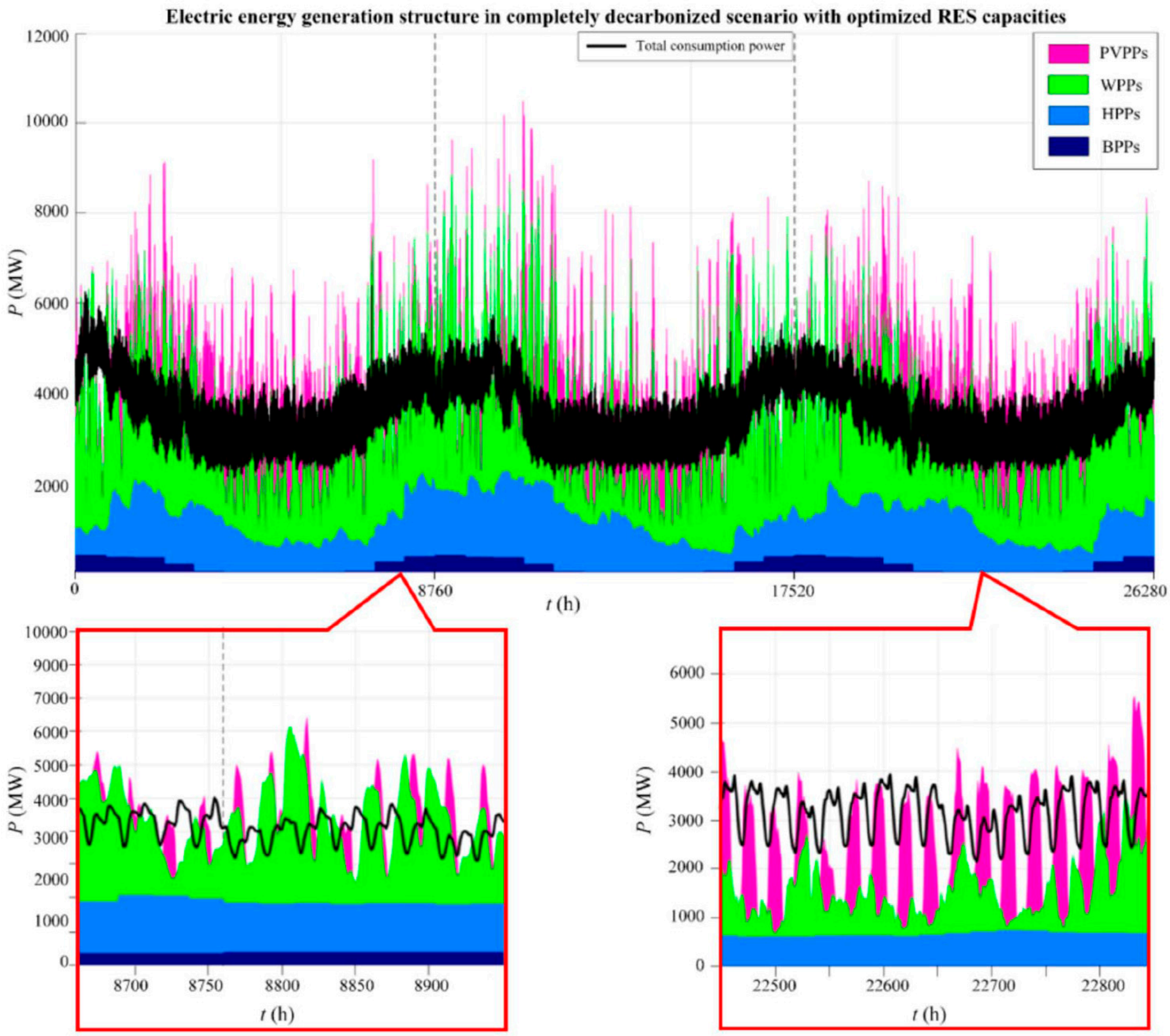


**Figure 8.** Different generation technology shares in the total generation profile.

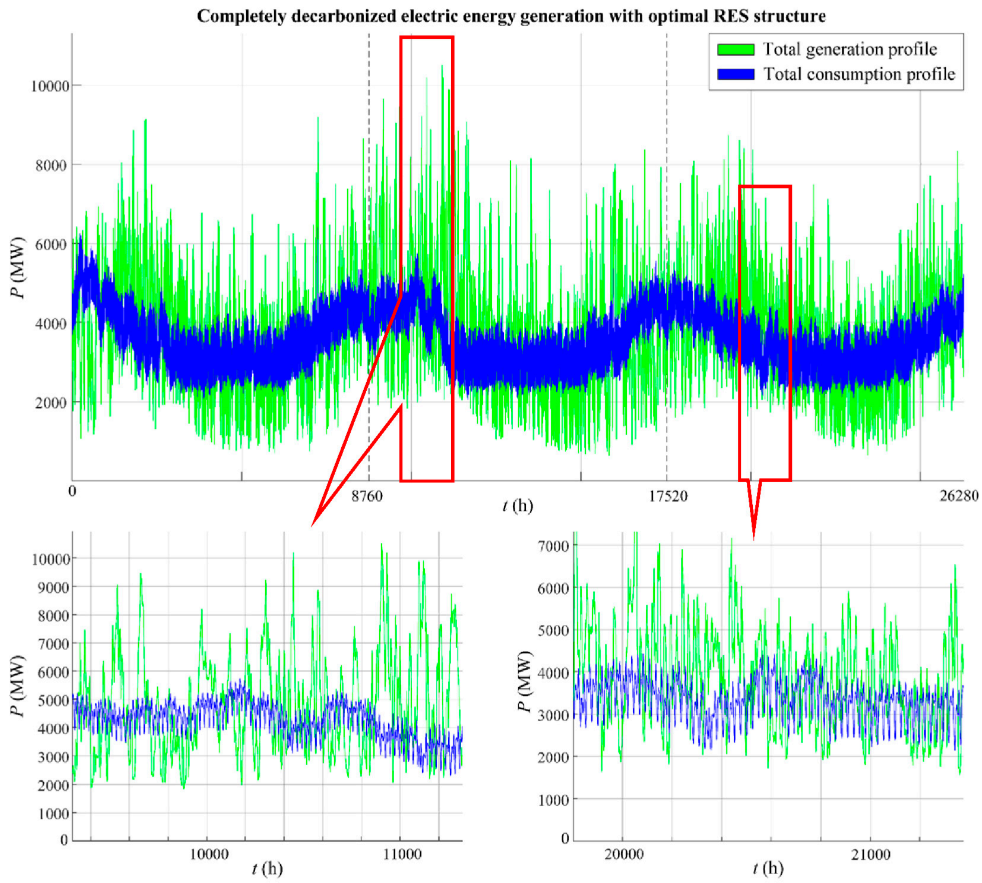


**Figure 9.** Total generation profile in completely decarbonized Serbian power system with optimized RES capacities.

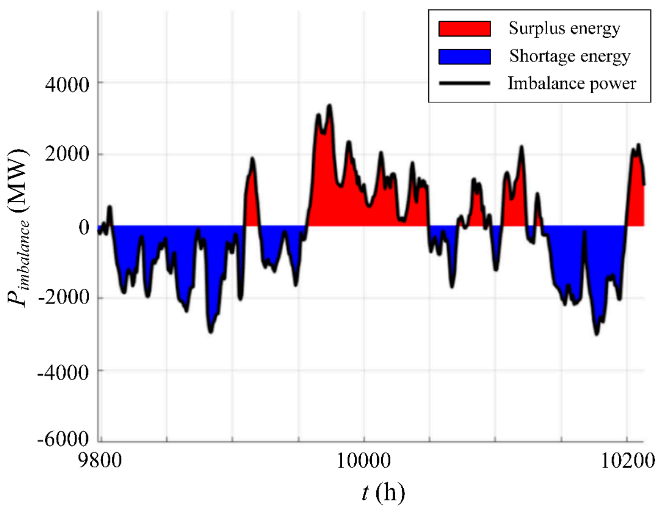


**Figure 10.** The imbalance power profile with surplus and shortage energy.

**Table 4.** The imbalance power profile characteristics for the analyzed three-year reference time period.

| Maximal Surplus Power (MW) | Maximal Surplus Power during 99% of the Time (MW) | Maximal Shortage Power (MW) | Maximal Shortage Power during 99% of the Time (MW) |
|---|---|---|---|
| 7096.9 | 4319.6 | 5070.6 | 4917.3 |

### 4.5. Discussion

Based on the performed calculations, it can be concluded that the complete decarbonization of electric energy generation in Serbia, requires the WPPs' capacity of 7088.7 MW, the utility-scale PVPPs' capacity of 3114.4 MW, the distributed PV capacity of 1940.7 MW, and the biogas CHPs' capacity of 180.5 MW to be installed. The optimal spatial allocation of the WPPs' and utility-scale PVPPs' capacities is given in Tables 1 and 2.

Efficient integration of the optimally dimensioned variable RES requires additional flexible capacities to be installed in the Serbian power system: energy storage systems and possibly flexible generating units also. These flexible capacities must provide the power profile which would compensate the difference between the total generation profile and the total consumption profile in the future decarbonized power system of Serbia. Before the assessment of the necessary structure and characteristics of the additional flexible capacities, the flexibility of the existing generating units (accumulation and run-of-the-river HPPs) should be engaged to reshape the imbalance power profile in order to reduce the required total installed power and energy storage capacity of the additional flexible capacities. This reshaping of the imbalance power profile should further reduce the sum of squared imbalance power, but the total energy generation in the power system will practically remain the same (differences will appear due to the nonlinear dependence of the HPP's output on the head and discharge, but the total amount of used water in HPPs is the same). This means that in the demonstrated case, the employment of the available flexibility of HPPs and controllable load in the Serbian power system would result in the amount of directly supplied consumption energy of more than 84.3%. Finally, knowing the reshaped imbalance power profile, different technology options for energy storage can be analyzed based on suitable economic and other criteria for helping investment decisions. Here, it is important to take into account that energy storage is accompanied by energy losses which depend on the storage technology applied. The energy lost due to storage has to be provided from additional generating units in the Serbian power system whose development has to be planned afterwards. Besides transmission network flexibility resources, significant resource for compensating the imbalance power is available on the consumption side, which can be activated through DSM system [91]. The capacity of controllable demand will be significantly increased through the expected integration of electric vehicles into distribution systems. Methods for spatio-temporal load forecasting in distribution networks with electric vehicles are developed [92] which provide day-ahead prediction of the flexibility capacity distribution system can provide in each hour. The system balancing on the consumption side is very economic and efficient because DSM does not require large investment costs, and its operation practically does not affect energy losses and does not create additional consumption of electric energy in the system, in contrast to the dedicatedly constructed energy storage in transmission network, such as pumped-hydro storage (PHS) or compressed air systems. Therefore, DSM should be utilized in the future to the greatest extent possible. Off course, inter-seasonal energy displacement will demand the existence of seasonal energy storages such as PHS and green hydrogen and ammonia, but their utilization for intra-day balancing of generation and consumption should be reduced to minimum through activating the more efficient DSM system.

Optimal dispatching of the available flexibility on both the generation and consumption sides can be realized through economic dispatching. A model for solving dynamic economic dispatch problems in a microgrid which contains traditional power generators, RES and energy storage devices is presented in [93]. Economic dispatching model can be extended to ensure low carbon dispatching of the integrated energy system as in [5,94].

The estimation of the maximal acceptable WPPs' and utility scale PVPPs' capacities that could be installed in a certain region took into account the regional capacity of the high voltage transmission network in terms of the maximal injected power which the network is able to evacuate from that region. The construction of the connecting lines and transformer stations is not included in the proposed model. These elements represent the missing power system infrastructure which should be planned during the process of development of each WPP and PVPP. The proposed model for the optimization of spatial allocation of WPPs' and PVPPs' capacities did not take into account the necessary power system infrastructure development and the transmission network losses corresponding to a certain RES development scenario. These aspects are envisaged to be analyzed by a separate calculation task after performing the proposed model. The perspective generation mixes that should be considered in these analyses correspond to the scenarios in the neighbourhood of the optimal scenario determined by the proposed model. This neighbourhood could be defined as a convex set surrounding the optimal solution in the way it was carried out in Section 4.5.1 when analysing the sensitivity of the optimal solution for the example of the Serbian power system. For each perspective generation mix, it is necessary to conduct a power system load flow and security study in order to determine the transmission network reinforcement needed to provide reliable energy supply from the generating capacities with the required power system security level and the acceptable level of transmission network losses. Therefore, the definition of the set of perspective scenarios enables to reallocate the planned WPPs' and PVPPs' capacities relative to the optimal allocation of these capacities in order to adjust the RES planning scenario to the transmission network, while having the acceptable deviation from the optimum which minimizes the flexibility requirements. This way it is possible to find the optimal RES planning scenario which would take into account both the effect of RES spatial allocation on the flexibility requirements and the effect of RES spatial allocation on the transmission network expansion and losses. When analyzing the necessary development of the missing transmission network infrastructure, as well as the exploitation of the existing transmission network, the dynamic thermal rating (DTR) system should be taken into account. This could provide the real transmission network capacity in windy areas to be significantly larger in comparison to the transmission network capacities calculated using static thermal models [95,96]. By applying the DTR system, the acceptable WPPs' capacities to be integrated can be significantly increased. When conducting the economic evaluation of the optimal solution and considering the necessary expansion and reinforcement of the transmission network, as well as the development and allocation of storage capacities, it is necessary to take care about the level of resilience of the electric power system. Besides energy independence, the resilience of electric power system is one of the imperatives of decarbonization process. One of the models for estimating the operating state of a perspective decarbonized power system regarding the evaluation of its resilience is proposed in [97].

The proposed model for the optimization of spatial allocation of WPPs' and PVPPs' capacities did not take into account the necessary power system infrastructure development and the transmission network losses corresponding to a certain RES development scenario. These aspects are envisaged to be analyzed by a separate calculation task after performing the proposed model. The perspective generation mixes that should be considered in these analyses correspond to the scenarios in the neighbourhood of the optimal scenario determined by the proposed model. This neighbourhood could be defined as a convex set surrounding the optimal solution in the way it was carried out in Section 4.5.1 when analysing the sensitivity of the optimal solution for the example of the Serbian power system. For each perspective generation mix, it is necessary to conduct a power system load flow and security study in order to determine the transmission network reinforcement needed to provide reliable energy supply from the generating capacities with the required power system security level and the acceptable level of transmission network losses. Therefore, the definition of the set of perspective scenarios enables to reallocate the planned WPPs' and PVPPs' capacities relative to the optimal allocation of these capacities in order to adjust the RES planning scenario to the transmission network, while having the acceptable deviation from the optimum which minimizes the flexibility requirements. This way it is possible to find the optimal RES planning scenario which would take into account both the effect of RES spatial allocation on the flexibility requirements and the effect of RES spatial allocation on the transmission network expansion and losses.

4.5.1. Sensitivity Analysis of the Optimal Solution

If, for any reason, the necessity arises to consider different RES developments in certain regions than the one obtained by model (1)–(5), it is important to know how much the deviation from the optimal solution will cost in terms of the change of directly supplied energy to consumers and in terms of the change of maximal imbalance power magnitude. In such cases, the planner can perform the calculation of model (1)–(5) with additional constraints requiring the installed capacities in certain regions to equal the desired values of the installed capacities. Here, we consider the RES development scenarios corresponding to the sum of squared errors which is not larger than the minimum for more than a certain percent, $p$, and investigate how much are the imbalance power profiles corresponding to these scenarios different from the optimum.

Since the criterion function (2a) is strictly convex and its domain is a convex set, it is possible to define a bounded convex set:

$$S(p) = \left\{ x \middle| f(x) = \|Ax - b\|_2^2 \leq \frac{100 + p(\%)}{100} f_{\min} \right\}, \tag{14}$$

where $f_{\min}$ is the minimum of the criterion function (2a) in model (1)–(5). Such set can be defined using any vectors $\Delta x^j$ which satisfy the condition:

$$f\left(x^{opt} + \Delta x^j\right) = \frac{100 + p(\%)}{100} f_{\min}, \tag{15}$$

in the following way:

$$S(p) = \left\{ x \middle| x = x^{opt} + \sum_j \alpha_j \Delta x^j, \alpha_j \geq 0, \sum_j \alpha_j \leq 1, f\left(x^{opt} + \Delta x^j\right) = \frac{100 + p(\%)}{100} f_{\min} \right\}. \tag{16}$$

Here, vector $x^{opt} = \left[x_1{}^{opt}, \ldots, x_{26}{}^{opt}\right]^{\mathrm{T}}$ is the solution to model (1)–(5) and its coordinates are optimal regional capacities of WPPs and utility scale PVPPs. Set $S(p)$ defined by (16) does not contain all vectors for which the relation (14) holds, but it is convenient to define it as the planner would be able to immediately recognize if a certain scenario belongs to the defined set. As function $f = \|Ax - b\|_2^2$ is strictly convex, it holds:

$$f(x) < \frac{100 + p(\%)}{100} f_{\min}, \ \forall x \in S, x \neq x^{opt} + \Delta x^j. \tag{17}$$

Thus, the function $f$ attains the largest value on set $S$ in $x = x^{opt} + \Delta x^j$. This means that, on set $S$, the imbalance profile $g(x) = Ax - b$ differs the most from $g_{opt} = Ax^{opt} - b$ in $x = x^{opt} + \Delta x^j$. In order to quantify how much is acceptable for a scenario $x$ to deviate from the optimum, we propose the following indicators: the maximal allowed decrease in the amount of directly supplied energy, $W_{directly\_supplied}(x)$, and the maximal allowed increase in the surplus power magnitude, $P_{surplus\_99\%}(x)$, which represents the maximal value of surplus power for 99% of the time. We want to find out how much the installed capacities can be changed with respect to the optimal values while having the mentioned indicators inside of the allowed ranges. In practice, different options for defining these ranges should be analyzed and the final choice should be supported by additional studies and economic considerations. Here, for the sake of discussion, we assume that in a scenario with a suitable imbalance profile the directly supplied energy should not decrease from the optimum for more than 1%, and that $P_{surplus\_99\%}(x)$ should not increase from the optimum for more than 1%. If for all $j$ holds:

$$W_{directly\_supplied}\left(x^{opt} + \Delta x^j\right) \geq 0.99 W_{directly\_supplied}(x_{opt}) \wedge \ P_{surplus\_99\%}\left(x^{opt} + \Delta x^j\right) \leq 1.01 P_{surplus\_99\%}(x_{opt}), \tag{18}$$

then these conditions probably hold for each $x \in S(p)$. In the following, we defined the set $S(p = 1\%)$ for which we verified this assumption for large number of randomly generated vectors from this set.

Vectors $\Delta x^j$ should be chosen in such way to describe both the range of possible increase and the range of possible decrease for all coordinates of vector $x^{opt}$. One possible choice of a set of vectors $\Delta x^j$ for which the criterion function increases 1% is shown in Figures 11 and 12. These vectors describe how much is possible to change the installed capacities from the optimal values and to have the sum of squared errors increased no more than 1%. For example, in the PVPPs' region 2 it was identified large technical potential for development of 3500 MW, but the optimal capacity mix allocated zero capacity in this region (Table 2). However, sensitivity analysis results given in Figure 12 show that even installing 1369.5 MW in PVPPs' region 2 would be acceptable to install if capacities in other regions change according to the values in column 32 in Figure 12. Similar considerations are possible for other regions. Similar considerations based on sensitivity analysis results are possible for all RES development scenarios that can be represented as linear combinations of vectors in Figures 11 and 12 in the following way:

$$x = x^{opt} + \sum_{j=1}^{33} \alpha_j \Delta x^j, \alpha_j \geq 0, \sum_{j=1}^{33} \alpha_j \leq 1. \tag{19}$$

Results in Figures 11 and 12 confirm that the capacities in the WPPs' regions: 1, 2, 4, 5, 7, 8, 15, 17–21 cannot be increased as their optimal values equal the maximal acceptable capacities in these regions. Additionally, the capacities in WPPs' regions: 3, 9, 12–14, and in PVPPs' region 2, cannot be decreased as their optimal values are zero or equal the already existing capacities in these regions.

| $\Delta x^j$ (MW) | | | | | | | | | | | | | | | | | | |
|---|---|---|---|---|---|---|---|---|---|---|---|---|---|---|---|---|---|---|
| COORDINATES \ *j* | 1 | 2 | 3 | 4 | 5 | 6 | 7 | 8 | 9 | 10 | 11 | 12 | 13 | 14 | 15 | 16 | 17 | 18 |
| 1 | 0 | 0 | 0 | 0 | 0 | 0 | 0 | 0 | 0 | 0 | −256.2 | 0 | 0 | 0 | 0 | 0 | 0 | 0 |
| 2 | 0 | 0 | 0 | 0 | 0 | 0 | 0 | 0 | 0 | 0 | 0 | −201.6 | 0 | 0 | 0 | 0 | 0 | 0 |
| 3 | 62.2 | 0 | 0 | 0 | 0 | 0 | 0 | 0 | 0 | 0 | 0 | 0 | 0 | 0 | 0 | 0 | 0 | 0 |
| 4 | 0 | 0 | 0 | 0 | 0 | 0 | 0 | 0 | 0 | 0 | 0 | 0 | −177.4 | 0 | 0 | 0 | 0 | 0 |
| 5 | 0 | 0 | 0 | 0 | 0 | 0 | 0 | 0 | 0 | 0 | 0 | 0 | 0 | −67.2 | 0 | 0 | 0 | 0 |
| 6 | 0 | 56.1 | 0 | 0 | 0 | 0 | 0 | 0 | 0 | 0 | 138.4 | 183.5 | 33.7 | 30.2 | −0.7 | −0.7 | 61.4 | −0.6 |
| 7 | 0 | 0 | 0 | 0 | 0 | 0 | 0 | 0 | 0 | 0 | 0 | 0 | 0 | 0 | 0 | −60.6 | 0 | 0 |
| 8 | 0 | 0 | 0 | 0 | 0 | 0 | 0 | 0 | 0 | 0 | 0 | 0 | 0 | 0 | 0 | 0 | −222.3 | 0 |
| 9 | 0 | 0 | 48.3 | 0 | 0 | 0 | 0 | 0 | 0 | 0 | 0 | 0 | 0 | 0 | 0 | 0 | 0 | 34.2 |
| 10 | 0 | 0 | 0 | 45.2 | 0 | 0 | 0 | 0 | 0 | 0 | −6.3 | 19.6 | 45.2 | −1.4 | −146.4 | −139.5 | −14.9 | −128.3 |
| 11 | 0 | 0 | 0 | 0 | 46.2 | 0 | 0 | 0 | 0 | 0 | 18.2 | 14.2 | 16.8 | 43.2 | −261.3 | −272.0 | 76.4 | −229.0 |
| 12 | 0 | 0 | 0 | 0 | 0 | 46.2 | 0 | 0 | 0 | 0 | 0 | 0 | 0 | 0 | 0 | 0 | 0 | 0 |
| 13 | 0 | 0 | 0 | 0 | 0 | 0 | 48.8 | 0 | 0 | 0 | 0 | 0 | 0 | 0 | 301.7 | 317.4 | 0 | 0 |
| 14 | 0 | 0 | 0 | 0 | 0 | 0 | 0 | 55 | 0 | 0 | 0 | 0 | 0 | 0 | 155.1 | 163.0 | 0 | 398.3 |
| 15 | 0 | 0 | 0 | 0 | 0 | 0 | 0 | 0 | 0 | 0 | 0 | 0 | 0 | 0 | 0 | 0 | 0 | 0 |
| 16 | 0 | 0 | 0 | 0 | 0 | 0 | 0 | 0 | 59.2 | 0 | 54.5 | −14.4 | 75.9 | 11.4 | −28.5 | −29.7 | 20.9 | −25.0 |
| 17 | 0 | 0 | 0 | 0 | 0 | 0 | 0 | 0 | 0 | 0 | 0 | 0 | 0 | 0 | 0 | 0 | 0 | 0 |
| 18 | 0 | 0 | 0 | 0 | 0 | 0 | 0 | 0 | 0 | 0 | 0 | 0 | 0 | 0 | 0 | 0 | 0 | 0 |
| 19 | 0 | 0 | 0 | 0 | 0 | 0 | 0 | 0 | 0 | 0 | 0 | 0 | 0 | 0 | 0 | 0 | 0 | 0 |
| 20 | 0 | 0 | 0 | 0 | 0 | 0 | 0 | 0 | 0 | 0 | 0 | 0 | 0 | 0 | 0 | 0 | 0 | 0 |
| 21 | 0 | 0 | 0 | 0 | 0 | 0 | 0 | 0 | 0 | 0 | 0 | 0 | 0 | 0 | 0 | 0 | 0 | 0 |
| 1 | 0 | 0 | 0 | 0 | 0 | 0 | 0 | 0 | 0 | 85.6 | 12.0 | 9.0 | 7.2 | 17.2 | −213.2 | 417.3 | 8.2 | −186.8 |
| 2 | 0 | 0 | 0 | 0 | 0 | 0 | 0 | 0 | 0 | 0 | 0 | 0 | 0 | 0 | 992.6 | 438.9 | 0 | 1071.0 |
| 3 | 0 | 0 | 0 | 0 | 0 | 0 | 0 | 0 | 0 | 0 | 25.4 | 9.3 | 25.4 | 18.1 | −247.1 | −257.3 | 33.7 | −415.8 |
| 4 | 0 | 0 | 0 | 0 | 0 | 0 | 0 | 0 | 0 | 0 | 6.9 | −3.0 | 4.3 | −7.0 | −144.2 | −150.1 | −7.8 | −126.3 |
| 5 | 0 | 0 | 0 | 0 | 0 | 0 | 0 | 0 | 0 | 0 | −2.6 | 1.5 | 1.3 | −1.0 | −301.5 | −313.9 | −8.1 | −264.2 |

**Figure 11.** Vectors describing the possible increase and decrease in regional capacities for which the sum of squared errors increases by no more than 1%.

| $\Delta x^j$ (MW) | | | | | | | | | | | | | | | | |
|---|---|---|---|---|---|---|---|---|---|---|---|---|---|---|---|---|
| | ***j*** | **19** | **20** | **21** | **22** | **23** | **24** | **25** | **26** | **27** | **28** | **29** | **30** | **31** | **32** | **33** |
| **COORDINATES** | **1** | 0 | 0 | 0 | 0 | 0 | 0 | 0 | 0 | 0 | 0 | 0 | 0 | 0 | 0 | 0 |
| | **2** | 0 | 0 | 0 | 0 | 0 | 0 | 0 | 0 | 0 | 0 | 0 | 0 | 0 | 0 | 0 |
| | **3** | 0 | 0 | 0 | 0 | 0 | 0 | 0 | 0 | 0 | 0 | 0 | 0 | 0 | 0 | 0 |
| | **4** | 0 | 0 | 0 | 0 | 0 | 0 | 0 | 0 | 0 | 0 | 0 | 0 | 0 | 0 | 0 |
| | **5** | 0 | 0 | 0 | 0 | 0 | 0 | 0 | 0 | 0 | 0 | 0 | 0 | 0 | 0 | 0 |
| | **6** | 0 | 0 | 0 | 0 | 92.3 | 104.4 | −0.5 | 8.0 | −0.6 | 89.9 | −2.3 | 12.2 | −0.3 | 34.8 | −0.7 |
| | **7** | 0 | 0 | 0 | 0 | 0 | 0 | 0 | 0 | 0 | 0 | 0 | 0 | 0 | 0 | 0 |
| | **8** | 0 | 0 | 0 | 0 | 0 | 0 | 0 | 0 | 0 | 0 | 0 | 0 | 0 | 0 | 0 |
| | **9** | 0 | 0 | 0 | 0 | 0 | 0 | 0 | 0 | 0 | 0 | 0 | 0 | 0 | 0 | 0 |
| | **10** | 0 | 0 | 0 | 0 | 220.7 | 124.3 | −109.2 | 11.6 | −122.8 | 11.8 | 40.2 | 15.0 | −70.4 | 9.5 | −151.4 |
| | **11** | 0 | 0 | 0 | 0 | −502.8 | 75.9 | −194.8 | 41.7 | −219.1 | 17.6 | 13.3 | 113.4 | −125.7 | 25.9 | −270.3 |
| | **12** | 0 | 0 | 0 | 0 | 0 | 0 | 0 | 0 | 0 | 0 | 0 | 0 | 0 | 0 | 0 |
| | **13** | 0 | 0 | 0 | 0 | 0 | 109.1 | 347.4 | 0 | 268.8 | 0 | 0 | 0 | 214.7 | 0 | 300.3 |
| | **14** | 0 | 0 | 0 | 0 | 23.9 | 600.0 | 0 | 0 | 148.8 | 0 | 0 | 0 | 294.3 | 0 | 75.2 |
| | **15** | 0 | 0 | 0 | 0 | 0 | −1417.8 | 0 | 0 | 0 | 0 | 0 | 0 | 0 | 0 | 0 |
| | **16** | 0 | 0 | 0 | 0 | 134.7 | 502.0 | −21.3 | 30.8 | −23.9 | 31.5 | 38.4 | 12.8 | −13.7 | 42.2 | 82.6 |
| | **17** | 0 | 0 | 0 | 0 | 0 | 0 | 0 | −87.0 | 0 | 0 | 0 | 0 | 0 | 0 | 0 |
| | **18** | 0 | 0 | 0 | 0 | 0 | 0 | 0 | 0 | −36.6 | 0 | 0 | 0 | 0 | 0 | 0 |
| | **19** | 0 | 0 | 0 | 0 | 0 | 0 | 0 | 0 | 0 | −127.2 | 0 | 0 | 0 | 0 | 0 |
| | **20** | 0 | 0 | 0 | 0 | 0 | 0 | 0 | 0 | 0 | 0 | −83.9 | 0 | 0 | 0 | 0 |
| | **21** | 0 | 0 | 0 | 0 | 0 | 0 | 0 | 0 | 0 | 0 | 0 | −151.0 | 0 | 0 | 0 |
| | **1** | 0 | 0 | 0 | 0 | 105.4 | 37.8 | −483.2 | 18.1 | −178.8 | 9.8 | 8.8 | 30.2 | −102.6 | −493.1 | −220.6 |
| | **2** | 87.4 | 0 | 0 | 0 | 0 | 0 | 1255.0 | 0 | 843.3 | 0 | 0 | 0 | 0 | 1369.5 | 1016.0 |
| | **3** | 0 | 85.6 | 0 | 0 | −51.0 | 32.9 | −184.3 | 24.0 | −207.2 | 17.2 | 11.1 | 28.4 | −118.9 | −571.6 | −255.6 |
| | **4** | 0 | 0 | 89.1 | 0 | 26.7 | −3.6 | −321.9 | −1.0 | −120.9 | −1.0 | 1.6 | −15.2 | −69.4 | 304.5 | −149.1 |
| | **5** | 0 | 0 | 0 | 81.8 | 59.4 | 48.9 | −224.8 | −5.7 | −252.8 | 1.0 | 6.4 | −24.6 | −145.0 | −697.2 | −311.8 |

**Figure 12.** Vectors describing the possible increase and decrease in regional capacities for which the sum of squared errors increases no more than 1%.

Larger deviations from the optimal scenario can be imposed by other practical limitations which were not taken into account by model (1)–(5). The installed capacities in certain regions may be turned to zero in case the network infrastructure development in those regions is too expensive. Additionally, it might be important to investigate the effect of greater development of RES in certain regions in order to align the targeted capacities with the interests of potential investors. These requirements can be added to model (1)–(5) as additional equality and inequality constraints. To help the analysis of such scenarios and reduce the number of extensive computations of model (1)–(5), the similarity between generation profiles of power plants in different regions is analyzed in the next section.

#### 4.5.2. Similarity between RES Generation in Different Regions

In real conditions of electric power system development in the process of decarbonization, it is very possible that, for different reasons, the targeted optimal capacity value of WPPs and PVPPs in some regions needs to be changed. These reasons could be economic or additional ecological constraints could be established or the estimation of the available resource could be corrected in some regions after conducting dedicated measurements. For practical applicability of the obtained optimal solution for spatial allocation of WPPs and PVPPs, it is necessary to analyze what is the best way to reallocate capacities of WPPs and PVPPs if a change of capacity of WPPs or PVPPs from the optimal value in certain region is necessary.

If the planner considers changing capacity in exactly one region, then from Figures 13 and 14, he can conclude what is the best way to reduce the deviation from the optimum by changing the installed capacities in other regions. These tables give the qualitative description of the relationship between the optimal changes of capacities in different regions (designated by black arrows) if the capacity in single region is changed (designated by red arrows). Blue fields in Figures 13 and 14 denote WPPs' regions, yellow fields denote PVPPs' regions. The numbers designate WPPs' and PVPPs' regions, and the numeration corresponds to Tables 1 and 2. At the intersection of each row $j$ and each column $i$ ($i \neq j$) in Figures 13 and 14, a black arrow is placed if a change of the capacity from the optimal value in region $i$ can compensate the effect of capacity change in region $j$. These arrows can have different sizes (the legend is shown in the lower left corner of Figures 13 and 14) which represents that the relative intensity of the capacity change from the optimal values is different in different regions. If the arrow in column $i$ is larger than the arrow in some other column, $k$, in the same row, this means that the required change of capacity from the optimal value in region $i$ is larger than the required change of capacity from the optimal value in region $k$. An upward directed arrow means that the compensation effect is accomplished by the increase in the capacity from the optimal value in the region corresponding to the column in which the arrow is placed. A downward directed arrow means that the compensation effect is accomplished by the decrease in the capacity from the optimal value in the region corresponding to the column in which the arrow is placed. The crossed red arrow in Figure 13 shows that the installed capacity in the region $j$ cannot be increased since its optimal value equals the upper boundary determined by the available area for constructing the power plants in that region. Similarly, in Figure 14, the crossed red arrow shows that the installed capacity in the region $j$ cannot be decreased since its optimal value equals the lower boundary.

For example, if there is an interest to increase the capacity of WPPs to be installed in region 7, then in order to achieve as small deviation as possible from the minimum value of the criterion function (2.1) (the sum of the squared errors), it would be needed to decrease the most the capacity of WPPs to be installed in region 16, the somewhat less decrease would occur in WPPs' regions 10 and 15, the even less decrease would happen in WPPs' region 11. The change of capacities in PVPPs' regions 1, 3 and 5 would be less than the change in WPPs' region 11, and the smallest change (practically insignificant) would occur in PVPPs' region 4. Figure 14 is created analogously for decreasing the installed capacity up to the lowest possible value which satisfies the constraints (2.2)–(2.4). If the planner needs to change the planned capacity in more than one region, Figures 13 and 14 will again give the set of regions in which capacities can be changed to reduce the deviation from the optimum, but the relative influence on these regions cannot be concluded from these tables.

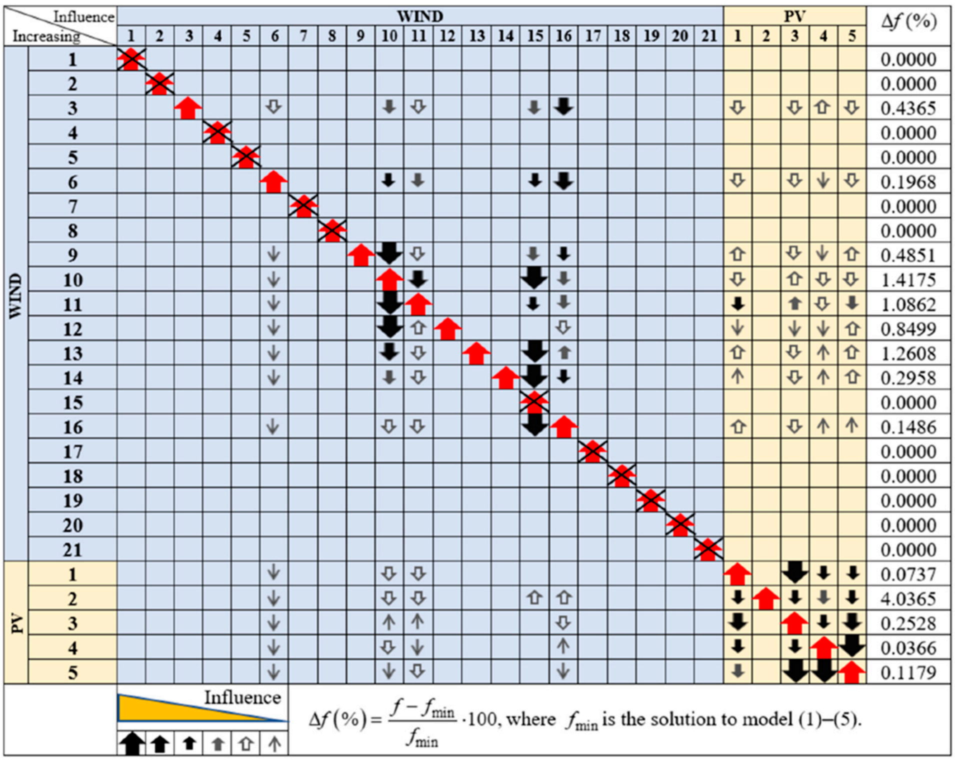


**Figure 13.** Means to reduce the effect on the sum of squared errors when increasing the capacity in exactly one region.

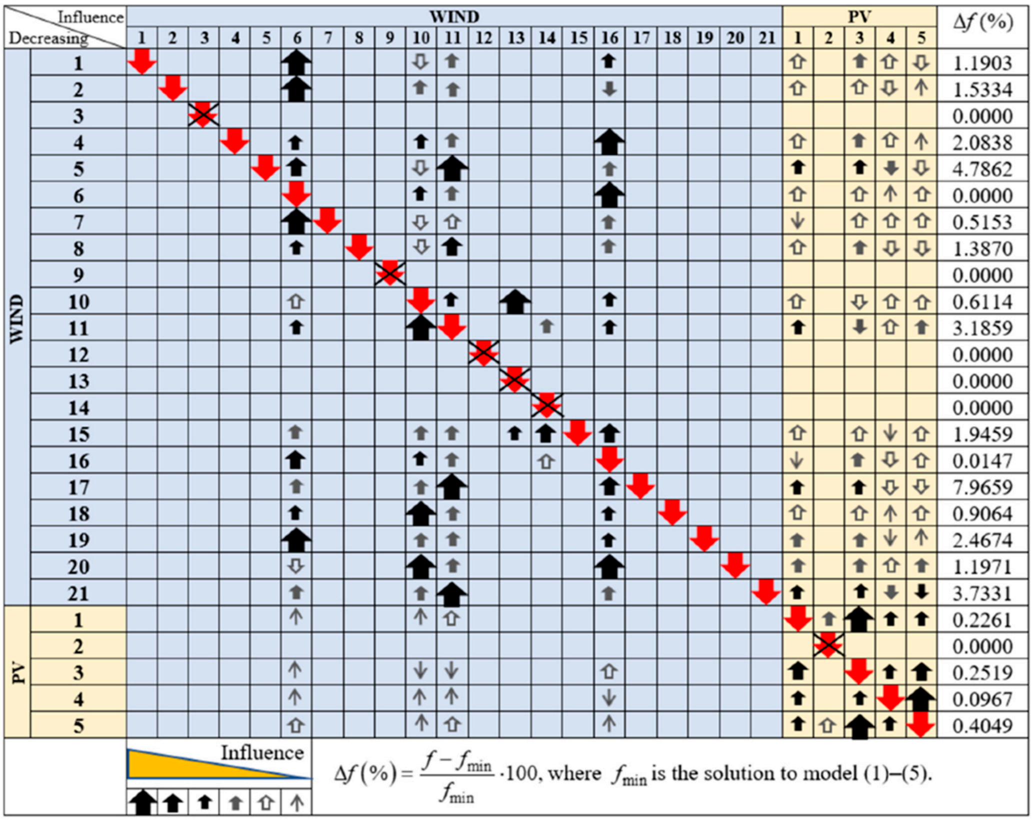


**Figure 14.** Means to reduce the effect on the sum of squared errors when decreasing the capacity in exactly one region.

In the last column of Figures 13 and 14 is shown the relative change of the criterion function (2.1) if the maximal acceptable change of the capacity in the region corresponding to the row is demanded. For example, according to the data in Table 2, in the region of central Serbia the maximal acceptable capacity for utility scale PVPPs is estimated to be 3500 MW. The proposed optimization model does not support the development of PVPPs in this region. If PVPPs of capacity 3500 MW instead of 0 would, nevertheless, be developed in this region, then, according to the data in Figure 13, it would be the most effective to reduce the optimal values of installed PVPPs' capacity in regions 1, 3 and 5 for the approximately equal amount, somewhat less reduction in the optimal capacity value should occur in PVPPs' region 4. The change of capacity should be approximately the same in WPPs' regions 10 (decreasing), 11 (decreasing), 15 (increasing) and 16 (increasing), and less than the capacity change in PVPPs' region 4. The smallest capacity reduction should occur in WPPs' region 6. In the remaining regions, the installed capacities should be kept on the optimal values, as calculated by model (1)–(5), which are shown in Tables 1 and 2. If these changes are applied in the optimal amounts, the criterion function would minimally deviate from the optimum. In this case, the increase in the criterion function would be 4.0365%; this information is given in the last column of Figure 13.

The results in Figures 13 and 14 reveal the positive correlation between specific generation profiles in different regions: if the increase in the capacity in the region $j$ can be compensated by a large decrease in the capacity in the region $i$. This way, regions with similar generation profiles can be identified, for example WPPs' region 9 is similar to WPPs' region 10 and WPPs' region 14 is similar to WPPs' region 15.

#### 4.5.3. Characterizing the Imbalance Profile Variability for a Certain RES Development Scenario

In order to represent the variability which characterizes the imbalance profile corresponding to a certain RES development scenario, we define the averaged effective balancing power related to a time period $T$,$P_{eff\_balancing}{}^{avg}(T)$, as follows:

$$P_{eff\_balancing}{}^{avg}(T) = \frac{1}{N_{periods}(T)} \sum_{j=1}^{N_{periods}(T)} P_{eff\_balancing\_j}(T), \quad (20)$$

$$P_{eff\_balancing\_j}(T) = \sqrt{\frac{1}{T} \sum_{k=k_{beginning\_j}}^{k_{ending\_j}} \left[P_{imbalance}(t_k) - P_{imbalance\_avg\_j}\right]^2 \cdot 1\mathrm{h}}, \quad (21)$$

$$P_{imbalance\_avg\_j} = \frac{1}{T} \sum_{k=k_{beginning\_j}}^{k_{ending\_j}} P_{imbalance}(t_k), \quad (22)$$

where $k_{beginning\_j}$ and $k_{ending\_j}$ are the first and the last hour of the $j^{th}$ period which duration is $T$ hours. The number of such periods in the considered time horizon of $N_h$ hours is $N_{periods}(T)$. The average of the imbalance power in the $j^{th}$ period is $P_{imbalance\_avg\_j}$. The deviation of the imbalance power from its centered moving average is used in (22) to calculate the effective balancing power, $P_{eff\_balancing\_j}(T)$. The effective balancing power defined this way represents the standard deviation of the imbalance power for a certain time period. Figure 15 shows the averaged effective balancing power depending on the duration of the period $T$. Characteristic values of this curve are:

- $P_{eff\_balancing}{}^{avg}(T = 24\text{ h}) = 961.2$ MW;
- $P_{eff\_balancing}{}^{avg}(T = 168\text{ h}) = 1323.6$ MW;
- $P_{eff\_balancing}{}^{avg}(T = 365/4 \cdot 24 = 2190\text{ h}) = 1673.8$ MW.

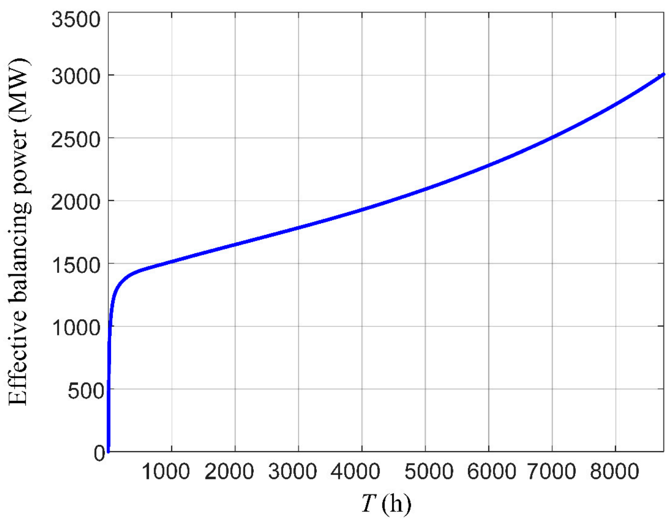


**Figure 15.** Characteristics of the imbalance profile variability in the optimal RES development scenario.

## 5. Conclusions

The proposed optimization model is demonstrated on the example of long-term RES development planning for complete decarbonization of electric energy generation in the Serbian power system which assumes the substitution of all the existing coal-fired thermal power plants by WPPs and PVPPs. It was shown that the optimal RES development planning according to the proposed methodology results in such structure and spatial allocation of WPPs and PVPPs which would provide more than 84% of consumption to be directly supplied from these sources without storage capacities. Demand side management and optimized operational planning of accumulation HPPs could further increase the amount of directly supplied consumption from RES in order to minimize the requirements for developing additional storage capacities.

The proposed model for the optimization of structure and spatial allocation of WPPs and PVPPs represents physical optimization, i.e., the adjustment of natural weather profiles of the primary resources (river flows, wind and irradiation) with the time profile of total electrical energy demand in the analyzed power system. It is based on LS method which makes the best use of the natural complementarity between wind, solar and hydro energy resources and their correlation with the total consumption profile in the future power system in order to achieve the best possible adjustment between the total generation profile and the total consumption profile. Besides maximizing the directly supplied consumption, the proposed model implicitly provides that the requirements from the additional flexibility capacities, which have to accompany the development of the RES, are simultaneously minimized which is of key importance for the stability of an electric power system. This also means that in general the energy that would have to pass through energy storage systems is minimized and, therefore, the required energy storage capacity and energy losses due to storage are minimized, whereas the required total installed power of storage systems is minimized, which reduces the investment costs and increases the power system energy efficiency.

The proposed model gives the best physical adjustment between the total generation and the total consumption profiles in the completely decarbonized electric power system and the attained optimum does not depend on any external factors (disruptions on the markets of primary energy sources and raw materials, wholesale electricity price, etc.). This optimization gives the highest level of electric power system independence and, indirectly, the highest reliability of electricity supply. The proposed model represents the basis for the economic optimization which should take into account economic aspects such as the cost of construction, operation and maintenance of RES capacities, costs for the development, reinforcement and exploitation of the transmission network, as well as the costs related to construction and exploitation of the balancing capacities. Economic aspects depend on market conditions and their long-term planning is not reliable, so it is necessary to conduct several phases of mid-term planning of WPPs and PVPPs in order to obtain the optimal spatial allocation of these plants. This optimum has significant flexibility, which is demonstrated on the example of the Serbian power system in Section 4.5.1. The flexibility of the optimal solution provides the possibility of performing additional optimizations in the surroundings of the optimal solution which take into account economic aspects and provide the minimal deviation from the physical optimum of the balance between the total generation and consumption profiles.

The proposed RES planning methodology could be used as a foundation for the development of the national energy strategy by serving as a guidance for defining capacity targets for regional capacity auctions in order to direct the investments in wind and solar power plants and achieve transition to dominantly renewable electricity production.

**Author Contributions:** Conceptualization, B.Š.; methodology, B.Š.; software, B.Š.; validation, B.Š.; formal analysis, B.Š.; investigation, B.Š.; resources, B.Š.; data curation, B.Š.; writing—original draft preparation, B.Š.; writing—review and editing, B.Š.; visualization, B.Š.; supervision, Ž.Đ. All authors have read and agreed to the published version of the manuscript.

**Funding:** This work was financially supported by the Ministry of Science, Technological Development and Innovation of the Republic of Serbia under contract number: 451-03-47/2023-01/200103.

**Data Availability Statement:** The wind speed measured data used to support the findings of this study are restricted by the Vortex company. Data on power plant production in Serbia and electricity consumption in Serbia are the property of Public Enterprise Electric Power Industry of Serbia and are available for researchers who meet the criteria for access to confidential data.

**Acknowledgments:** Authors thank the company Vortex FDC for providing us the necessary wind resource data and the Ministry of Science, Technological Development and Innovation of the Republic of Serbia for financial support under contract number: 451-03-47/2023-01/200103.

**Conflicts of Interest:** The authors declare no conflict of interest.

## Nomenclature

| | |
|---|---|
| WPP | Wind power plant |
| PVPP | Photovoltaic power plant |
| RES | Renewable energy sources |
| TPP | Thermal power plant |
| PV | Photovoltaic |
| ESOM | Energy system optimization model |
| MGA | Modelling to generate alternatives |
| ETEM | Energy technology environment model |
| RE | Renewable energy |
| LS | Least squares |
| HPP | Hydroelectric power plant |
| LDP | Least distance programming |
| NNLS | Nonnegative least squares |
| CHP | Combined heat and power |
| BPP | Biogas power plant |
| IPA | Important plant areas |
| IBA | Important bird areas |
| PBA | Prime butterfly areas |

## List of Symbols

| | |
|---|---|
| $A$ | The system matrix |
| $P_{WPPspec\_j}(t_k)$ | The specific generation of WPPs in region $j$ in the $k^{th}$ hour of the referent planning period. |
| $P_{PVspec\_i}(t_k)$ | The specific generation of PVPPs in region $i$ in the $k^{th}$ hour of the referent planning period. |
| $N_h$ | The number of hours in the referent planning period. |
| $N$ | The number of years in the referent planning period. |
| $N_{WPP}$ | The number of regions with technically exploitable wind potential. |
| $N_{PV}$ | The number of regions with technically exploitable PV potential. |
| $P_{WPPnom\_j}$ | The installed capacity (rated power) of WPPs in region $j$. |
| $P_{PVnom\_j}$ | The installed capacity (rated power) of PVPPs in region $j$. |
| $x^{\min}$ | The column vector of capacities of already existing WPPs and PVPPs in the analyzed regions |
| $x^{\max}$ | The column vector of maximal acceptable installed capacities of WPPs and PVPPs in the analyzed regions. |
| $P_{ref\_load}(t_k)$ | The referent consumption power in the $k^{th}$ hour of the referent planning period. |
| $P_{distPVtot}(t_k)$ | The total distributed PV generation power in the $k^{th}$ hour of the referent planning period. |
| $b$ | The column vector which elements are the differences between the referent consumption power and the total distributed PV generation power in each hour of the referent time period, chronologically ordered. |
| ${N_h}^m$ | The number of hours in the $m^{th}$ year of the referent time period. |
| $h^m$ | The difference between the energy of the referent consumption profile and the total generated energy from distributed PV in the $m^{th}$ year of the referent time period. |
| $G_m$ | The row vector which elements are the total energy produced by unit capacity of WPPs or PVPPs in analyzed regions during the $m^{th}$ year of the referent time period. |
| $W_{WAsP\_j}$ | The expected annual energy generation for the representative wind turbine of WPPs in region $j$. |
| $V_{ji}$ | Wind speed measured at the representative wind turbine mast height in the $i^{th}$ hour in the region $j$. |
| $\rho_{ji}$ | Air density measured at the representative wind turbine mast height in the $i^{th}$ hour in the region $j$. |
| $V_{eff\_j}(t_i)$ | The effective wind speed at the representative wind turbine mast height in the $i^{th}$ hour in the region $j$. |
| $\rho_0$ | The standard air density. |
| $\eta_j$ | The scaling coefficient for region $j$. |
| $P_{power\_curve\_j}\left(\eta_j V_{eff\_j}(t_i)\right)$ | The value of power on the power curve of the representative wind turbine corresponding to the value of wind speed equal to $\eta_j V_{eff\_j}(t_i)$. |
| $N_{dist}$ | The number of distribution networks. |

| | |
|---|---|
| $P_{distPV\_i}{}^{spec}$ | The specific PV generation profile for the $i^{th}$ distribution network. |
| $y_{J\_i}$ | The relative reduction in Joule's losses in the $i^{th}$ distribution network. |
| $R_{eq\_i}$ | The equivalent resistance which models the total Joule's losses in the $i^{th}$ distribution network. |
| $P_{load\_i}(t_k)$ | The active power measured at the high voltage side of the transformation station which supplies the $i^{th}$ distribution network in the $k^{th}$ hour. |
| $Q_{load\_i}(t_k)$ | The reactive power measured at the high voltage side of the transformation station which supplies the $i^{th}$ distribution network in the $k^{th}$ hour. |
| $U_{n\_i}$ | The rated RMS voltage at the high voltage side of the transformation station which supplies the $i^{th}$ distribution network. |
| $c_{1i}$, $c_{2i}$ | Coefficients for calculating the relative reduction in Joule's losses in the $i^{th}$ distribution network which would be achieved by installing the distributed PV capacity $x_{dist\_i}$ in that network. |
| $y_{J\_i}{}^{\max}$ | The maximal relative reduction in Joule's losses in the $i^{th}$ distribution network. |
| $x_{dist\_i}{}^{opt}$ | The installed capacity of distributed PV systems in the the $i^{th}$ distribution network which would result In the maximal relative reduction in Joule's losses in that network. |
| $y_J{}^{target}$ | The target value of the relative reduction in Joule's losses which the planner attempts to exactly or approximately achieve in each distribution network. |
| $x_{dist\_i}{}^{planned}$ | The distributed PV capacity planned to be installed in the $i^{th}$ distribution network. |
| $y_{J\_achieved}{}^{avg}$ | The weighted average value of the achieved Joule's losses reduction in all distribution networks. |
| $P_{distPVnom\_tot}$ | The total capacity of distributed PV systems planned to be installed in all distribution networks. |
| $S(p)$ | A bounded convex set of RES development scenarios scenarios in the neighbourhood of the optimal scenario, for which the criterion function is no more than $p$ percent larger than the minimum. |
| $p$ | The percentage increase in the criterion function relative to the optimal value |
| $\Delta x^j$ | The $j^{the}$ vector in the set of vectors chosen to define the set $S(p)$. |
| $\alpha_j$ | The $j^{the}$ coefficient in the set of coefficients which describe exactly one scenario $x$ in the set $S(p)$ |
| $x^{opt}$ | The vector which coordinates are the optimal capacities of WPPs and PVPPs obtained by solving the model (1)–(5). |
| $x_i{}^{opt}$ | The $i^{th}$ coordinate of the vector $x^{opt}$. |
| $f$ | The criterion function in the model (1)–(5). |
| $f_{\min}$ | The optimal value of the criterion function in the model (1)–(5). |
| $g(x)$ | The vector which elements are the imbalance power corresponding to the RES development scenario $x$, In each hour of the referent time period, chronologically ordered. |
| $W_{directly\_supplied}(x)$ | The amount of directly supplied energy corresponding to the RES development scenario $x$. |
| $P_{surplus\_99\%}(x)$ | The surplus power magnitude which represents the maximal value of surplus power for 99% of the time, corresponding to the RES development scenario $x$. |

## References


1. International Energy Agency. *World Energy Outlook 2022—An Updated Roadmap to Net Zero Emissions by 2050*; International Energy Agency: Paris, France, 2022.
2. Tong, D.; Zhang, Q.; Zheng, Y.; Caldeira, K.; Shearer, C.; Hong, C.; Qin, Y.; Davis, S.J. Committed emissions from existing energy infrastructure jeopardize 1.5 °C climate target. *Nature* **2019**, *572*, 373–377. [CrossRef] [PubMed]
3. Luderer, G.; Krey, V.; Calvin, K.; Merrick, J.; Mima, S.; Pietzcker, R.; Van Vliet, J.; Wada, K. The role of renewable energy in climate stabilization: Results from the EMF27 scenarios. *Clim. Chang.* **2014**, *123*, 427–441. [CrossRef]
4. International Energy Agency. *Coal in Net Zero Transitions: Strategies for Rapid, Secure and People-Centred Change*; International Energy Agency: Paris, France, 2022.
5. Zhang, L.; Liu, D.; Cai, G.; Lyu, L.; Koh, L.H.; Wang, T. An optimal dispatch model for virtual power plant that incorporates carbon trading and green certificate trading. *Int. J. Electr. Power Energy Syst.* **2023**, *144*, 108558. [CrossRef]
6. Bukowski, M.; Majewski, J.; Sobolewska, A. The Environmental Impact of Changes in the Structure of Electricity Sources in Europe. *Energies* **2023**, *16*, 501. [CrossRef]
7. REN21. *Renewables 2022 Global Status Report*; REN21: Paris, France, 2022.
8. Global Wind Energy Council. *Global Wind Report 2022*; Global Wind Energy Council: Brussels, Belgium, 2022.
9. Solar Power Europe. *Global Market Outlook for Solar Power 2022–2026*; Solar Power Europe: Brussels, Belgium, 2022.
10. Heptonstall, P.J.; Gross, R.J.K. A systematic review of the costs and impacts of integrating variable renewables into power grids. *Nat. Energy* **2021**, *6*, 72–83. [CrossRef]
11. Nyenah, E.; Sterl, S.; Thiery, W. Pieces of a puzzle: Solar-wind power synergies on seasonal and diurnal timescales tend to be excellent worldwide. *Environ. Res. Commun.* **2022**, *4*, 055011. [CrossRef]
12. Sterl, S.; Liersch, S.; Koch, H.; van Lipzig, N.P.M.; Thiery, W. A new approach for assessing synergies of solar and wind power: Implications for West Africa. *Environ. Res. Lett.* **2018**, *13*, 094009. [CrossRef]

13. Strbac, G.; Aunedi, M. *Whole-System Cost of Variable Renewables in Future GB Electricity System*; Joint Industry Project with RWE Innogy, Renewable Energy Systems and Scottish Power Renewables, E3G; Imperial College of London: London, UK, 2016.
14. Verástegui, F.; Lorca, Á.; Olivares, D.; Negrete-Pincetic, M. Optimization-based analysis of decarbonization pathways and flexibility requirements in highly renewable power systems. *Energy* **2021**, *234*, 121242. [CrossRef]
15. Sepulveda, N.A.; Jenkins, J.D.; de Sisternes, F.J.; Lester, R.K. The role of firm low-carbon electricity resources in deep decarbonization of power generation. *Joule* **2018**, *2*, 2403–2420. [CrossRef]
16. Scott, I.J.; Carvalho, P.M.; Botterud, A.; Silva, C.A. Clustering representative days for power systems generation expansion planning: Capturing the effects of variable renewables and energy storage. *Appl. Energy* **2019**, *253*, 113603. [CrossRef]
17. Feijoo, F.; Pfeifer, A.; Herc, L.; Groppi, D.; Duić, N. A long-term capacity investment and operational energy planning model with power-to-X and flexibility technologies. *Renew. Sustain. Energy Rev.* **2022**, *167*, 112781. [CrossRef]
18. Geem, Z.W.; Kim, J.H. Optimal Energy Mix with Renewable Portfolio Standards in Korea. *Sustainability* **2016**, *8*, 423. [CrossRef]
19. Cho, S.; Kim, H.; Lee, S.; Kim, S.; Jeon, E.-C. Optimal energy mix for greenhouse gas reduction with renewable energy—The case of the South Korean electricity sector. *Energy Environ.* **2020**, *31*, 1055–1076. [CrossRef]
20. Huang, M.C.; Kim, C.J. Investigating Cost-Effective Policy Incentives for Renewable Energy in Japan: A Recursive CGE Approach for an Optimal Energy Mix. *Singap. Econ. Rev.* **2021**, *66*, 507–528. [CrossRef]
21. Dehghan, H.; Nahavandi, N.; Chaharsooghi, S.K.; Zarei, J.; Amin-Naseri, M.R. A hybrid game theory and system dynamics model to determine optimal electricity generation mix. *Comput. Chem. Eng.* **2022**, *166*, 107990. [CrossRef]
22. Yu, S.; Zhou, S.; Zheng, S.; Li, Z.; Liu, L. Developing an optimal renewable electricity generation mix for China using a fuzzy multi-objective approach. *Renew. Energy* **2019**, *139*, 1086–1098. [CrossRef]
23. Gómez-Calvet, R.; Martínez-Duart, J.M.; Serrano-Calle, S. Current state and optimal development of the renewable electricity generation mix in Spain. *Renew. Energy* **2019**, *135*, 1108–1120. [CrossRef]
24. Babonneau, F.; Barrera, J.; Toledo, J. Decarbonizing the Chilean Electric Power System: A Prospective Analysis of Alternative Carbon Emissions Policies. *Energies* **2021**, *14*, 4768. [CrossRef]
25. Simon, S.; Naegler, T.; Gils, H.C. Transformation towards a Renewable Energy System in Brazil and Mexico—Technological and Structural Options for Latin America. *Energies* **2018**, *11*, 907. [CrossRef]
26. Zozmann, E.; Göke, L.; Kendziorski, M.; Angel, C.; Hirschhausen, C.; Winkler, J. 100% Renewable Energy Scenarios for North America—Spatial Distribution and Network Constraints. *Energies* **2021**, *14*, 658. [CrossRef]
27. Potashnikov, V.; Golub, A.; Brody, M.; Lugovoy, O. Decarbonizing Russia: Leapfrogging from Fossil Fuel to Hydrogen. *Energies* **2022**, *15*, 683. [CrossRef]
28. Hirth, L.; Ueckerdt, F.; Edenhofer, O. Integration costs revisited—An economic framework for wind and solar variability. *Renew. Energy* **2015**, *74*, 925–939. [CrossRef]
29. Palmintier, B.S.; Webster, M.D. Impact of operational flexibility on electricity generation planning with renewable and carbon targets. *IEEE Trans. Sustain. Energy* **2016**, *7*, 672–684. [CrossRef]
30. Poncelet, K.; Delarue, E.; D'haeseleer, W. Unit commitment constraints in long term planning models: Relevance, pitfalls and the role of assumptions on flexibility. *Appl Energy* **2020**, *258*, 113843. [CrossRef]
31. Hua, B.; Baldick, R.; Wang, J. Representing operational flexibility in generation expansion planning through convex relaxation of unit commitment. *IEEE Trans. Power Syst.* **2018**, *33*, 2272–2281. [CrossRef]
32. Zhang, L.; Capuder, T.; Mancarella, P. Unified unit commitment formulation and fast multi-service lp model for flexibility evaluation in sustainable power systems. *IEEE Trans. Sustain. Energy* **2015**, *7*, 658–671. [CrossRef]
33. Palmintier, B.S.; Webster, M.D. Heterogeneous Unit Clustering for Efficient Operational Flexibility Modeling. *IEEE Trans. Power Syst.* **2014**, *29*, 1089–1098. [CrossRef]
34. Jenkins, J.D.; Sepulveda, N.A. *Enhanced Decision Support for a Changing Electricity Landscape: The GenX Configurable Electricity Resource Capacity Expansion Model*; MITEI-WP-2017-10; MIT Energy Initiative: Cambridge, MA, USA, 2017.
35. Mai, T.; Barrows, C.; Lopez, A.; Hale, E.; Dyson, M.; Eurek, K. *Implications of Model Structure and Detail for Utility Planning: Scenario Case Studies Using the Resource Planning Model*; Technical Report NREL/TP-6A20-63972; National Renewable Energy Lab: Golden, CO, USA, 2015.
36. Aghaei, J.; Amjady, N.; Baharvandi, A.; Akbari, M.-A. Generation and transmission expansion planning: MILP–based probabilistic model. *IEEE Trans. Power Syst.* **2014**, *29*, 1592–1601. [CrossRef]
37. Mallapragada, D.S.; Papageorgiou, D.J.; Venkatesh, A.; Lara, C.L.; Grossmann, I.E. Impact of model resolution on scenario outcomes for electricity sector system expansion. *Energy* **2018**, *163*, 1231–1244. [CrossRef]
38. Dranka, G.G.; Ferreira, P.; Vaz, A.I.F. A review of co-optimization approaches for operational and planning problems in the energy sector. *Appl. Energy* **2021**, *304*, 117703. [CrossRef]
39. Drechsler, M.; Egerer, J.; Lange, M.; Masurowski, F.; Meyerhoff, J.; Oehlmann, M. Efficient and equitable spatial allocation of renewable power plants at the country scale. *Nat. Energy* **2017**, *2*, 17124. [CrossRef]
40. Lohr, C.; Schlemminger, M.; Peterssen, F.; Bensmann, A.; Niepelt, R.; Brendel, R.; Hanke-Rauschenbach, R. Spatial concentration of renewables in energy system optimization models. *Renew. Energy* **2022**, *198*, 144–154. [CrossRef]
41. Lombardi, F.; Pickering, B.; Colombo, E.; Pfenninger, S. Policy decision support for renewables deployment through spatially explicit practically optimal alternatives. *Joule* **2020**, *4*, 2185–2207. [CrossRef]

42. Sasse, J.P.; Trutnevyte, E. Distributional trade-offs between regionally equitable and cost-efficient allocation of renewable electricity generation. *Appl. Energy* **2019**, *254*, 113724. [CrossRef]
43. Sasse, J.P.; Trutnevyte, E. Regional impacts of electricity system transition in Central Europe until 2035. *Nat. Commun.* **2020**, *11*, 4972. [CrossRef]
44. Brown, T.; Hörsch, J.; Schlachtberger, D. PyPSA: Python for Power System Analysis. *J. Open Res. Softw.* **2018**, *6*, 4. [CrossRef]
45. Berntsen, P.B.; Trutnevyte, E. Ensuring diversity of national energy scenarios: Bottom up energy system model with modeling to generate alternatives. *Energy* **2017**, *126*, 886–898. [CrossRef]
46. Lund, H.; Arler, F.; Østergaard, P.A.; Hvelplund, F.K.; Connolly, D.; Mathiesen, B.V.; Karnøe, P. Simulation versus Optimisation: Theoretical Positions in Energy System Modelling. *Energies* **2017**, *10*, 840. [CrossRef]
47. Senatla, M.; Bansal, R.C. Review of planning methodologies used for determination of optimal generation capacity mix: The cases of high shares of PV and wind. *IET Renew. Power Gener.* **2018**, *12*, 1222–1233. [CrossRef]
48. Available online: https://www.energyplan.eu/ (accessed on 27 March 2023).
49. Available online: https://iea-etsap.org/index.php/etsap-tools/model-generators/times (accessed on 27 March 2023).
50. Available online: http://www.osemosys.org/ (accessed on 27 March 2023).
51. Available online: https://www.energyexemplar.com/plexos (accessed on 27 March 2023).
52. Fripp, M. Switch: A planning tool for power systems with large shares of intermittent renewable energy. *Environ. Sci. Technol.* **2012**, *46*, 6371–6378. [CrossRef]
53. Available online: http://www.gurobi.com (accessed on 27 March 2023).
54. Available online: https://h2res.org/ (accessed on 27 March 2023).
55. Palisade Corporation. *Evolver*; Palisade Corporation: Ithaca, NY, USA, 2016.
56. Cheng, C.; Blakers, A.; Stocks, M.; Lu, B. 100% renewable energy in Japan. *Energy Convers. Manag.* **2022**, *255*, 115299. [CrossRef]
57. Lu, B.; Blakers, A.; Stocks, M.; Cheng, C.; Nadolny, A. A zero-carbon, reliable and affordable energy future in Australia. *Energy* **2021**, *220*, 119678. [CrossRef]
58. Luz, T.; Moura, P. 100% Renewable energy planning with complementarity and flexibility based on a multi-objective assessment. *Appl. Energy* **2019**, *255*, 113819. [CrossRef]
59. Brown, P.R.; Botterud, A. The value of inter-regional coordination and transmission in decarbonizing the US electricity system. *Joule* **2021**, *5*, 115–134. [CrossRef]
60. Aghahosseini, A.; Bogdanov, D.; Breyer, C. Towards sustainable development in the MENA region: Analysing the feasibility of a 100% renewable electricity system in 2030. *Energy Strategy Rev.* **2020**, *28*, 100466. [CrossRef]
61. Navia, M.; Orellana, R.; Zaráte, S.; Villazón, M.; Balderrama, S.; Quoilin, S. Energy Transition Planning with High Penetration of Variable Renewable Energy in Developing Countries: The Case of the Bolivian Interconnected Power System. *Energies* **2022**, *15*, 968. [CrossRef]
62. Thangavelu, S.R.; Khambadkone, A.M.; Karimi, I.A. Long-term optimal energy mix planning towards high energy security and low GHG emission. *Appl. Energy* **2015**, *154*, 959–969. [CrossRef]
63. Anasis, J.G.; Khalil, M.A.K.; Butenhoff, C.; Bluffstone, R.; Lendaris, G.G. Optimal energy resource mix for the US and China to meet emissions pledges. *Appl. Energy* **2019**, *238*, 92–100. [CrossRef]
64. Anasis, J.G.; Khalil, M.A.K.; Butenhoff, C.; Bluffstone, R.; Lendaris, G.G. A Combined Energy and Geoengineering Optimization Model (CEAGOM) for climate and energy policy analysis. *Appl. Energy* **2018**, *218*, 246–255. [CrossRef]
65. Carraro, C.; Tavoni, M.; Longden, T.; Marangoni, G. *The Optimal Energy Mix in Power Generation and the Contribution from Natural Gas in Reducing Carbon Emissions to 2030 and Beyond*; CESIFO Working Peper NO. 4432 Category 10: Energy and Climate Economics; SSRN: Rochester, NY, USA, 2013.
66. Aryanpur, V.; O'Gallachoir, B.; Dai, H.; Chen, W.; Glynn, J. A review of spatial resolution and regionalisation in national-scale energy systems optimisation models. *Energy Strategy Rev.* **2021**, *37*, 100702. [CrossRef]
67. Göke, L. AnyMOD.jl: A Julia package for creating energy system models. *SoftwareX* **2021**, *16*, 100871. [CrossRef]
68. Breyer, C.; Bogdanov, D.; Gulagi, A.; Aghahosseini, A.; Barbosa, L.S.N.S.; Koskinen, O.; Barasa, M.; Caldera, U.; Afanasyeva, S.; Child, M.; et al. On the role of solar photovoltaics in global energy transition scenarios. *Prog. Photovolt. Res. Appl.* **2017**, *25*, 727–745. [CrossRef]
69. Das, P.; Kanudia, A.; Bhakar, R.; Mathur, J. Intra-regional renewable energy resource variability in long-term energy system planning. *Energy* **2022**, *245*, 123302. [CrossRef]
70. Maimó-Far, A.; Homar, V.; Tantet, A.; Drobinski, P. The effect of spatial granularity on optimal renewable energy portfolios in an integrated climate-energy assessment model. *Sustain. Energy Technol. Assess.* **2022**, *54*, 102827. [CrossRef]
71. Gils, H.C.; Simon, S.; Soria, R. 100% Renewable Energy Supply for Brazil—The Role of Sector Coupling and Regional Development. *Energies* **2017**, *10*, 1859. [CrossRef]
72. Lugovoy, O.; Jyothiprakash, V.; Chatterjee, S.; Sharma, S.; Mukherjee, A.; Das, A.; Some, S.; Dinesha, D.L.; Das, N.; Bosu, P.; et al. Towards a Zero-Carbon Electricity System for India in 2050: IDEEA Model-Based Scenarios Integrating Wind and Solar Complementarity and Geospatial Endowments. *Energies* **2021**, *14*, 7063. [CrossRef]
73. Aghahosseini, A.; Bogdanov, D.; Breyer, C. A Techno-Economic Study of an Entirely Renewable Energy-Based Power Supply for North America for 2030 Conditions. *Energies* **2017**, *10*, 1171. [CrossRef]

74. Jurasz, J.; Canales, F.A.; Kies, A.; Guezgouz, M.; Beluco, A. A review on the complementarity of renewable energy sources: Concept, metrics, application and future research directions. *Sol. Energy* **2020**, *195*, 703–724. [CrossRef]
75. Björck, Å. Chapter 5 Constrained Least Squares Problems. In *Numerical Method for Least Squares Problems*; SIAM: Philadelphia, PA, USA, 1995; pp. 194–197.
76. Cline, A.K. *The Transformation of a Quadratic Programming Problem into Solvable Form*; Tech. Report ICASE 75-14; NASA, Langley Research Center: Hampton, VA, USA, 1975.
77. Lawson, C.L.; Hanson, R.J. *Solving Least Squares Problems*; Prentice-Hall: Englewood Cliffs, NJ, USA, 1974; pp. 154–196.
78. Haskell, K.H.; Hanson, R.J. Algorithm for linear least squares problems with equality and nonnegativity constraints. *Math Program.* **1981**, *21*, 98–118. [CrossRef]
79. Available online: https://www.mathworks.com/ (accessed on 27 March 2023).
80. Elektroprivreda Srbije. *Annual Technical Reports for Years 2016–2021*; Elektroprivreda Srbije: Belgrade, Serbia, 2021. (In Serbian)
81. Ministry of Environmental Protection of the Republic of Serbia, Environmental Protection Agency. *Annual Report on the State of Air Quality in Republic of Serbia in 2021*; Ministry of Environmental Protection of the Republic of Serbia: Belgrade, Serbia, 2022.
82. Institute for Nature Conservation of Serbia. Official Map of Protected Areas. Available online: https://cloud.gdi.net/visios/zzps (accessed on 27 March 2023).
83. Republic Geodetic Authority of Serbia. National Spatial Data Infrastructure. Available online: https://a3.geosrbija.rs/ (accessed on 27 March 2023).
84. NASA's Eearth Observing System. Shuttle Radar Topography Mission Data. Available online: https://dwtkns.com/srtm30m/ (accessed on 27 March 2023).
85. European Copernicus Land Monitoring Service. Corine Land Cover Data. Available online: https://land.copernicus.eu/pan-european/corine-land-cover (accessed on 27 March 2023).
86. Available online: https://www.wasp.dk/ (accessed on 27 March 2023).
87. Ministry Agriculture, Forestry and Water Management of Serbia. Portal for the Classification of State Land. Available online: https://gp.upz.minpolj.gov.rs/visios/GPpublic (accessed on 27 March 2023).
88. SARAH Solar Radiation Data, EU Science Hub (europa.eu). Available online: https://ec.europa.eu/jrc/en/PVGIS/downloads/SARAH (accessed on 27 March 2023).
89. Available online: https://globalsolaratlas.info/download/serbia (accessed on 27 March 2023).
90. Serbian Biogas Association, Ministry of Agriculture, Forestry and Water Economy of the Republic of Serbia. *Biogas Power Plants Guide for Investment*; Serbian Biogas Association: Novi Sad, Serbia, 2020.
91. Kotur, D.; Đurišić, Ž. Optimal spatial and temporal demand side management in a power system comprising renewable energy sources. *Renew. Energy* **2017**, *108*, 533–547. [CrossRef]
92. Huang, N.; He, Q.; Qi, J.; Hu, Q.; Wang, R.; Cai, G.; Yang, D. Multinodes interval electric vehicle day-ahead charging load forecasting based on joint adversarial generation. *Int. J. Electr. Power Energy Syst.* **2022**, *143*, 108404. [CrossRef]
93. Duan, Y.; Zhao, Y.; Hu, J. An initialization-free distributed algorithm for dynamic economic dispatch problems in microgrid: Modeling, optimization and analysis. *Sustain. Energy Grids Netw.* **2023**, *34*, 101004. [CrossRef]
94. Liu, G.; Qin, Z.; Diao, T.; Wang, X.; Wang, P.; Bai, X. Low carbon economic dispatch of biogas-wind-solar renewable energy system based on robust stochastic optimization. *Int. J. Electr. Power Energy Syst.* **2022**, *139*, 108069. [CrossRef]
95. Su, Y.; Teh, J. Two-Stage Optimal Dispatching of AC/DC Hybrid Active Distribution Systems Considering Network Flexibility. *J. Mod. Power Syst. Clean Energy* **2023**, *11*, 52–65. [CrossRef]
96. Poučković, B.; Đurišić, Ž. Current carrying capacity of overhead line that connects wind power plant to the grid. In Proceedings of the 10th International Conference on Environment and Electrical Engineering (EEEIC), Rome, Italy, 8–11 May 2011; ISBN 978-1-4244-8779-0.
97. Wang, H.; Wang, B.; Luo, P.; Ma, F.; Zhou, Y.; Mohamed, M.A. State Evaluation Based on Feature Identification of Measurement Data: For Resilient Power System. *CSEE J. Power Energy Syst.* **2021**, *8*, 983–992. [CrossRef]